COMPLEXITY AND SPACE PLASMAS

George Pavlos
Democritus University of Thrace
Department of Electrical and Computer Engineering
Xanthi, Greece

HELLENIC ASTRONOMICAL SOCIETY

The 11th Hellenic Astronomical Conference

8-12 September 2013, Athens

European Union
European Social Fund

OPERATIONAL PROGRAMME
EDUCATION AND LIFELONG LEARNING
investing in knowledge society
MINISTRY OF EDUCATION, LIFELONG LEARNING AND RELIGIOUS AFFAIRS
MANAGING AUTHORITY

NSRF 2007-2013
programme for development
EUROPEAN SOCIAL FUND

Co- financed by Greece and the European Union

History A

1984

Weiss N.O., et al., Periodic and aperiodic dynamo waves, Geoph. & Astroph. Fluid Dynamics, 30, 305-345, 1984.

1985

Ruzmaikin A.A., The solar dynamo, Solar Phys. 100, 125-140,1985.

Spiegel E.A., Cosmic Arrhythmias, in Chaos in astrophysics; Proceedings of the Advanced Research Workshop, Palm Coast, FL, Dordrecht, D. Reidel Publishing Co., p. 91-135, 1985.

1986

Kurths J. And Herzel H., Can a solar pulsation event be characterized by a low – dimensional chaotic attractor?, Solar Physics 107, 39-45, 1986.

1987

Buchner J. and Zelenyi L.M., Chaotization of the electron motion as the cause of an internal magnetotail instability and substorm onset, J. Geophys. Res., 92, A12, 13456, 1987.

1988

Pavlos G.P., Magnetospheric Dynamics, Proc.Symposium on Solar and Space Physics, ed. D. Dialetis, p.1-43,National Observatory of Athens, 1988.

Pavlos, G.P., Magnetospheric Dynamics and Chaos theory, Hellenic Physical Society, Athens,1988.

1989

Buchner J. and Zelenyi L.M., Regular and chaotic charged particle motion in magnetotaillike field reversals: 1. Basic theory of trapped motion, J. Geophys. Res., 94, A9, 11821, 1989.

Weiss N.O., In Accretion discs and magnetic fields in Astrophysics, ed. G. Belvedere, Kluwer, Dordrecht, 1989.

1990

Weiss N.O., Periodicity and aperiodicity in solar magnetic activity, Phil. Trans. R. Soc. Lond., A 330, 617, 1990.

Baker D.N., et al., The evolution from weak to strong geomagnetic activity: an interpretation in terms of deterministic chaos, Geophys. Res. Lett., 17, 41, 1990.

Vassiliadis D., et al., Low dimensional chaos in magnetospheric activity from AE time series, Geophys. Res. Lett., 17, 841, 1990.

History B

1991

Pavlos et al., Chaotic dynamics in Astrophysics and Space Physics, Proc. 1st General Confernece of the Balkan Physical Union, Thessaloniki, 1991.

Pavlos G.P., et al., Evidence for strange attractor structure in space plasmas, Ann. Geophysicae, 10, 309-322, 1991.

Voros Z., Synergetic Approach to Substorm Phenomenon, Magnetospheric Substorms, Geophysical Monograph 64, American Geophysical Union, 1991.

Burlaga L.F., Multifractal structure in the interplanetary magnetic field, Geophys. Res. Lett., 18, 69, 1991.

1992

Pavlos G.P., et al., Evidence for chaotic dynamics in the outer solar plasma and the earth magnetosphere, Chaotic dynamics: Theory and Practice, ed. Bountis T., Plenum Press, New York, 1992.

Pavlos G.P., et al., A preliminary low-dimensional chaotic analysis of the solar cycle, Ann. Geophysicae, 10, 759-762, 1992.

Chang T., Low-dimensional behavior and symmetry breaking of stochastic systems near criticality-can these effects be observed in space and in the laboratory?, Plasma Science, IEEE, 20, 691-694, 1992.

1994

Pavlos G.P., et al., Chaos and magnetospheric dynamics, Non. Proc. Geophys., 1, 124-135, 1994.

1999

Pavlos, G.P., et al., Comments and new results about the magnetospheric chaos hypothesis, Non. Proc. Geophys., 6, 99-127, 1999.

Chang T., Self-organized criticality, multi-fractal spectra, sporadic localized reconnections and intermittent turbulence in the magnetotail, Phys. Plasma, 6, 4137, 1999.

2011

Pavlos G.P., et al., First and second order non-equilibrium phase transition and evidence for non-extensive Tsallis statistics in Earth's magnetosphere, Physica A, 390, 2819-2839, 2011.

2012

Pavlos G.P., et al., Tsallis statistics and magnetospheric self-organization, Physica A, 391, 3069-3080, 2012.

Pavlos et al., Tsallis non-extensive statistics, intermittent turbulence, SOC and chaos in the solar plasma, Part one: Sunspot dynamics, Physica A 391 (2012) 6287–6319.

2013

Karakatsanis, L., **Pavlos G.,** Xenakis, M.Tsallis non-extensive statistics, intermittent turbulence, SOC and chaos in the solar plasma. Part two: Solar Flares dynamics, Physica A, 2012.

Pavlos et all. (2013) Universality of Tsallis Non - Extensive Statistics and Time Series Analysis: accepted for publication in Physica A.

Physical Theory from Past to Future

Mechanistic reductionism, microscopical causality
(from bottom to top)

Holistic multiscale distributed causality
(from bottom to top and from top to bottom)

Irreversibility of time, novelty and creativity

DRIVEN SYSTEMS (LOADING - UNLOADING)
Solar Dynamics

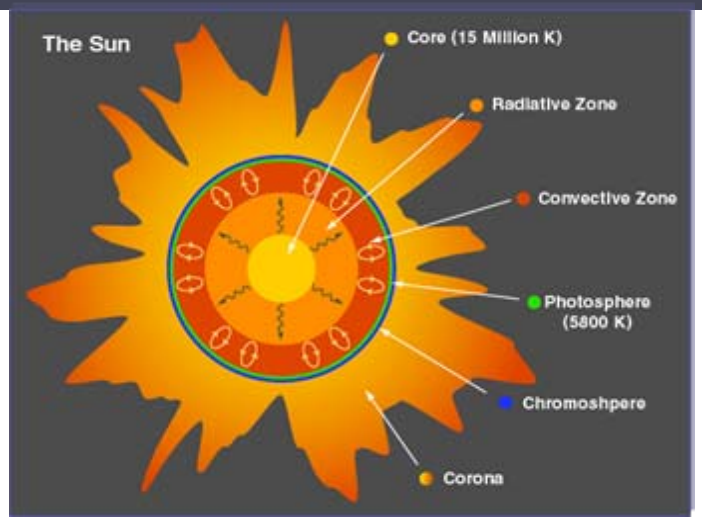

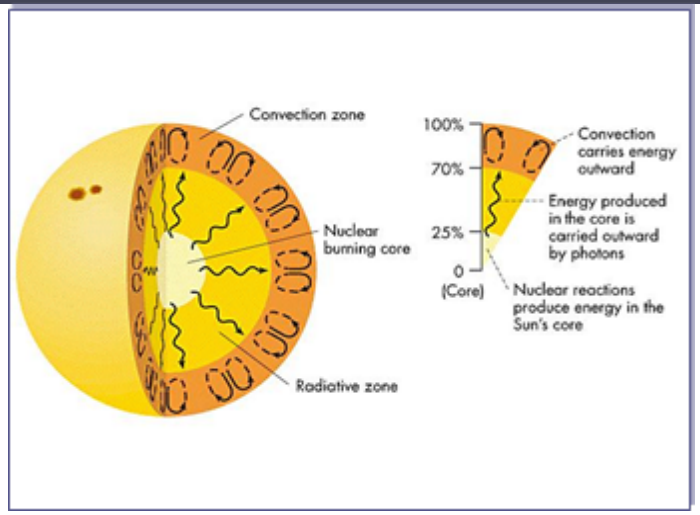

Description of Sun's Interior

Input (Solar

SunSpots
Prominence
Flares

Driven System (Photosphere)

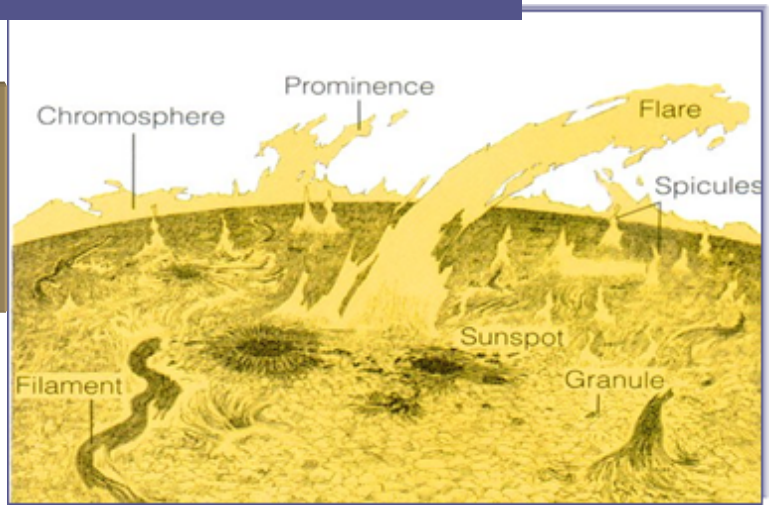

Description of Sun's Photosphere

Solar Wind

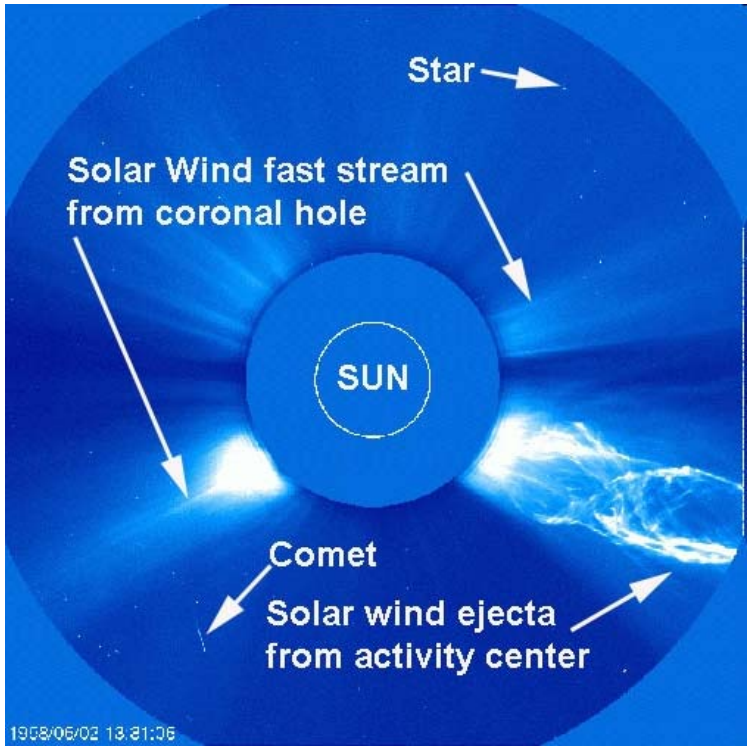
Star
Solar Wind fast stream
from coronal hole
SUN
Comet
Solar wind ejecta
from activity center
1998/06/02 13:31:06

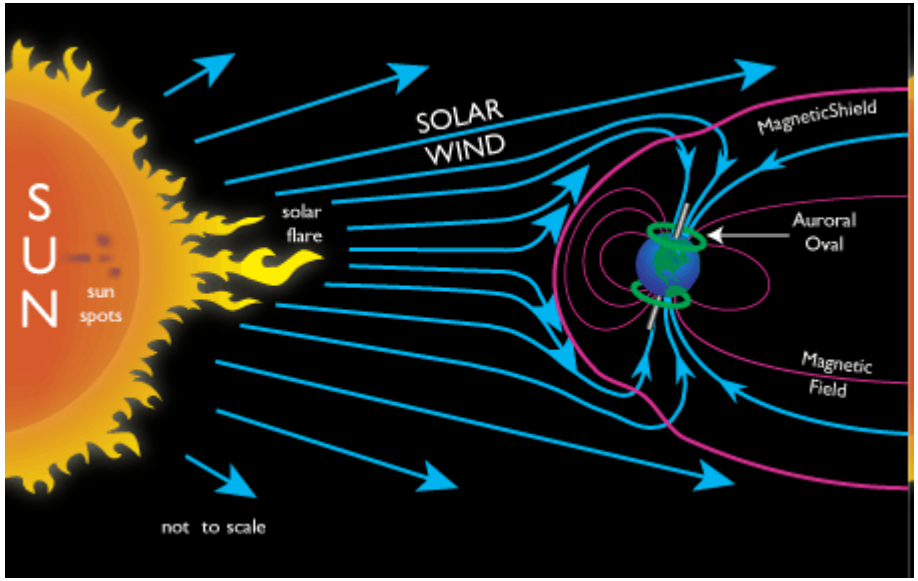
SOLAR
WIND
MagneticShield
Auroral
Oval
S
U
N
sun
spots
solar
flare
Magnetic
Field
not to scale

MAGNETOSPHERIC SYSTEM

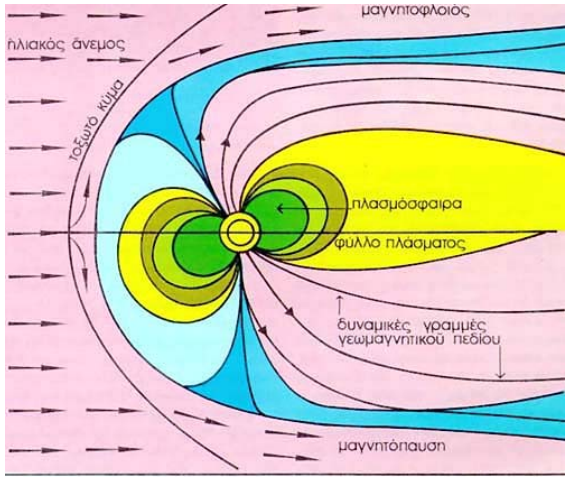

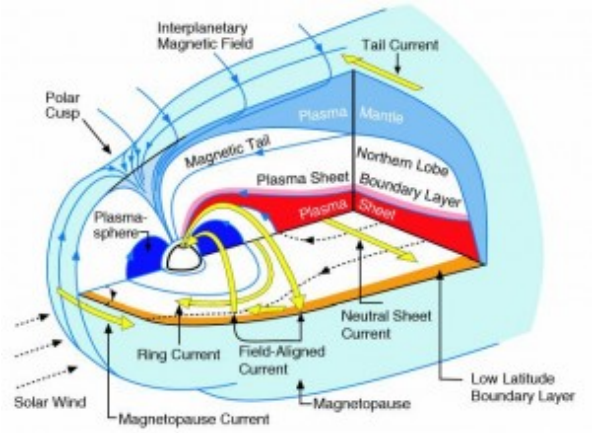

INPUT
SOLAR WIND

DRIVEN SYSTEM
MAGNETOSPHERE

OUTPUT
MAGNETOSPHERIC SUBSTORMS

SPACE PLASMAS AND MODERN CONCEPTS FROM COMPLEXITY THEORY

- Fractal and Multifractal structures (Mandelbrot, 1982; Grassberger & Procaccia, 1984; P Halsey, 1987)
- Non-extensive statistical mechanics (Tsallis, 1988)
- Fractal topology (Alexander and Orbach, 1982; Zelenyi and Milovanov, 2004)
- Turbulence – Intermittence Turbulence theory (Kolmogorov, 1941; Mandelbrot, 1999; Frisch,1996)
- Strange kinetics - dynamics (Shlesinger, Zaslavsky & Klafter, 1993)
- Percolation theory (Stanley, 1984; Havlin, 1984; Stauffer, 1985;Isichenko, 1992; Milovanov, 1997)
- Anomalous diffusion theory and anomalous transport theory (Montroll, 1981; Shlesinger, Zaslavsky & Klafter,1993; Milovanov, 2001)
- Fractional dynamics (Leibniz, Liouville, Riemman, Weyl; Procaccia, 1985; Mainardi, 1997; Tarasov, 2013)
- Non-equilibrium phase transition theory (Chang, 1992).

CHAOTIC ALGORITHM

Takens Theorem (1981)

State Space Reconstruction

ORIGINAL STATE SPACE

συνθήκη: $m \geq 2D+1$

EMBEDDING

RECONSTRUCTED STATE SPACE

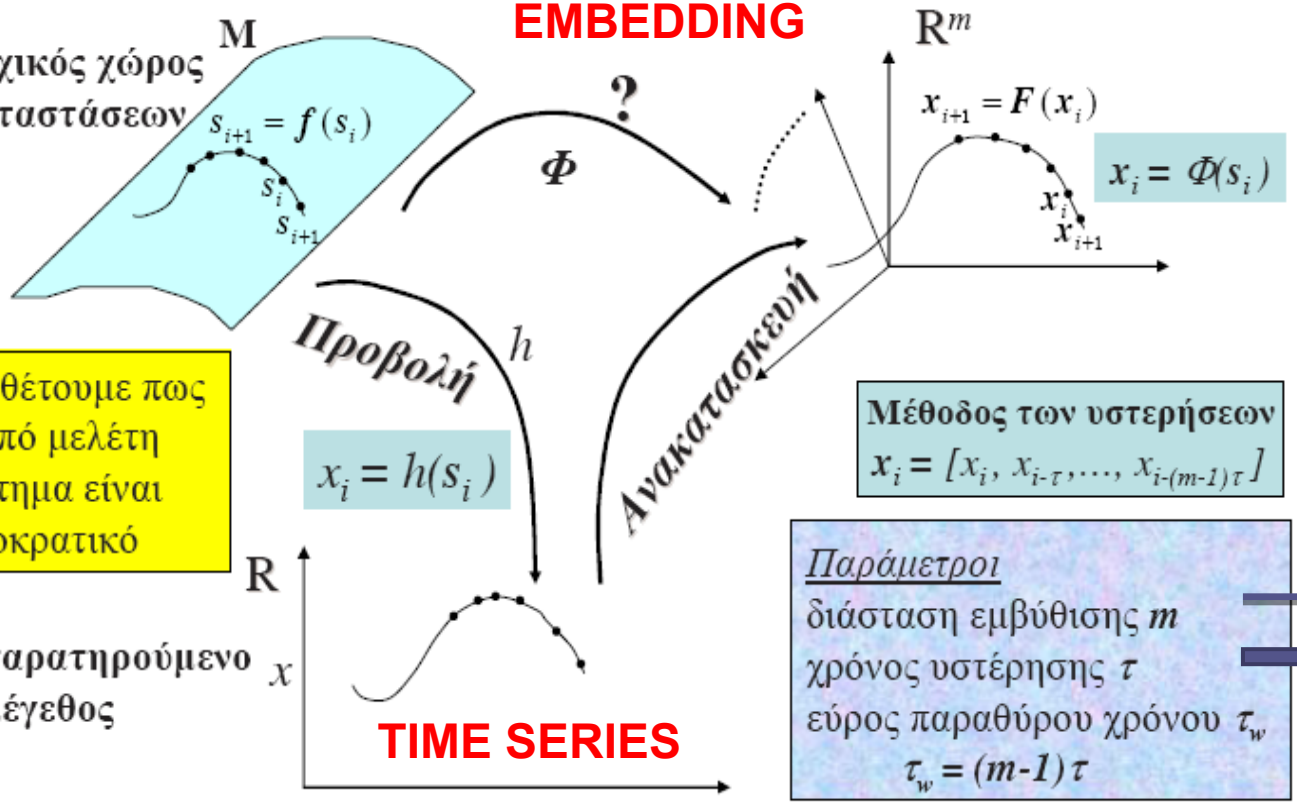

Υποθέτουμε πως το υπό μελέτη σύστημα είναι αιτιοκρατικό

Μέθοδος των υστερήσεων

$x_i = [x_i, x_{i-\tau}, \ldots, x_{i-(m-1)\tau}]$

Παράμετροι

διάσταση εμβύθισης m

χρόνος υστέρησης τ

εύρος παραθύρου χρόνου τ_w

$\tau_w = (m-1)\tau$

- ✓ m μικρό, αυτοτομές
- ✓ m μεγάλο, θόρυβος

- ✓Αυτοσυσχέτιση
- ✓ Αμοιβαία Πληροφορία

The Chaotic Algorithm is based in proficient mathematical concepts: **Embedding theory, metrics, fractals, multiple manifolds, probability – information theory, dynamical systems and maps**

Σημειώσεις: Δ. Κουγιουμτζής

FLOW CHART OF CHAOTIC ALGORITHM

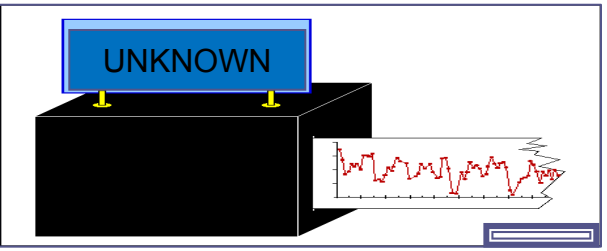

Local Data = Timeseries

Reconstructed Phase Space

– SVD analysis

Phenomenological Characteristics

Dynamic Degrees of Freedom

Dynamic Instability

Chaos – SOC - Turbulence

Test of Null Hypothesis

Linearity – Non-Linearity - Noise

Non-Linear Prediction Models

Spatiotemporal Modeling

Law of Internal Dynamics

$$\frac{d\mathbf{X}}{dt} = \mathbf{F}(\mathbf{X}(t), \mathbf{u}(t), \lambda, w(t))$$

SYNOPSIS

Chaotic Analysis
Dimensional Analysis

Statistical Analysis

Turbulence Analysis

Non – Linear Physics

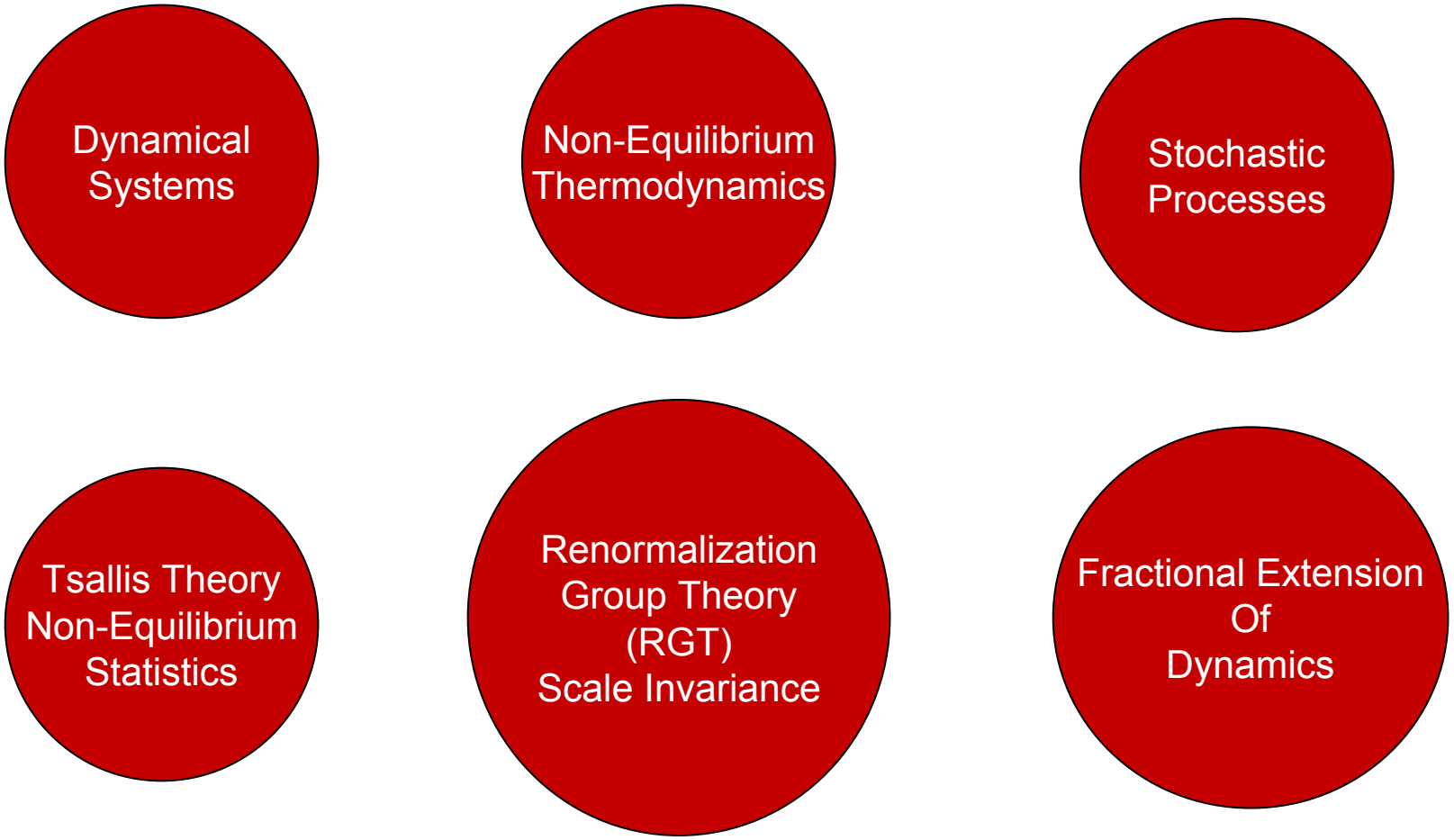

Tsallis Extension of Statistics

Nonextensive Statistical Mechanics

Microscopic Level → Macroscopic Level

Quantum Complexity
Quantum Phase Transition
(Q.P.T.)

Equilibrium Phase Transition
(E.P.T.)

Non – Equilibrium
Phase Transition
(N.E.P.T.)

Dynamical Bifurcation

$$dx/dt = f(x,\lambda)$$

Non – Linear Dynamics

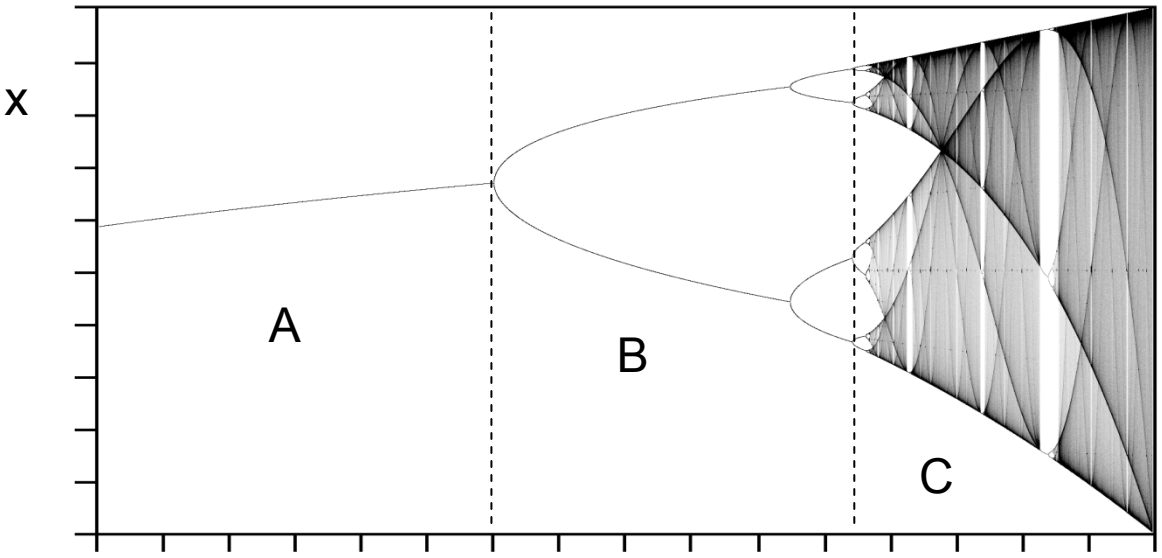

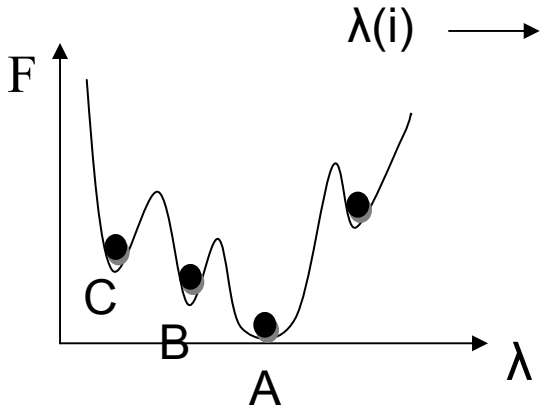

Critical Points
Bifurcation Points

(A)
Gaussian Equilibrium
Critical States
Equilibrium Phase Transition
Power Laws

(B)
Self-Organization Structure
Dissipative Structures
Long Range Correlations

(C)
Low Dimensional Chaos
Strange Attractors
Turbulence
Spatiotemporal Chaos
Scale Invariance
SOC
Intermittent Turbulence
Non Gaussian Prob.
Fractal Dynamics

SELF ORGANIZED CRITICALITY

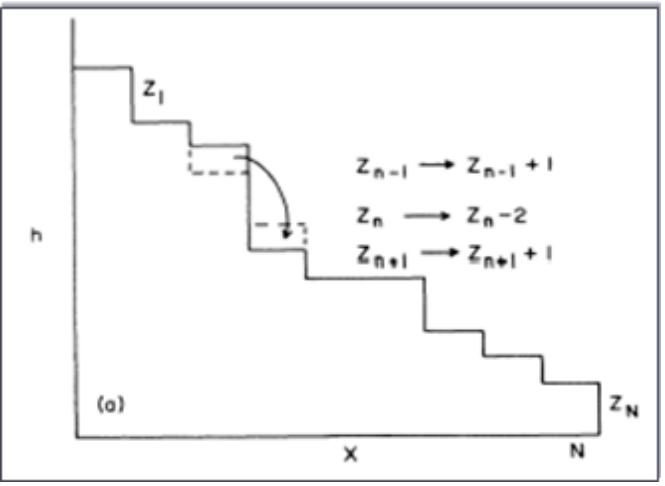

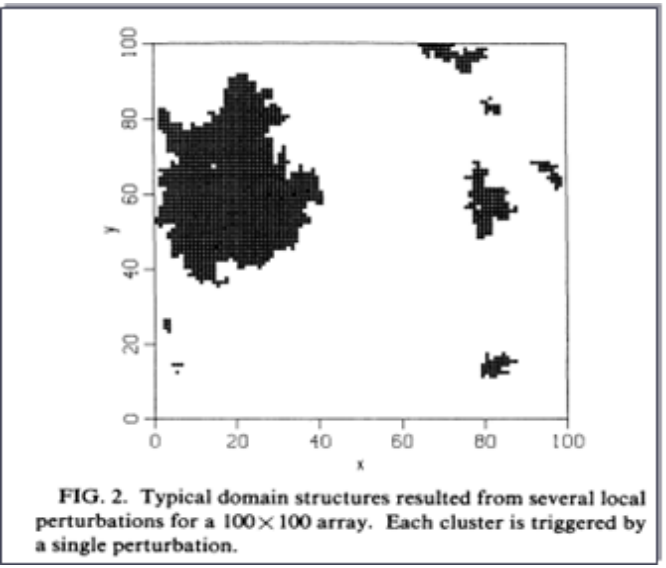

FIG. 2. Typical domain structures resulted from several local perturbations for a 100×100 array. Each cluster is triggered by a single perturbation.

In SOC systems the uncertainty grows with time much more slowly than does with chaotic systems. The uncertainty increases according to a **power law**, rather than an exponential law. The system evolves on the border of chaos. This behavior called **"weak chaos"** is a result of self organized criticality.

Dissipative Dynamical Systems with extended spatial degrees of freedom and local interacting evolve into self organized critical states.

(Per Bak, 1988)

1 / f "noise" – power law scaling

Space

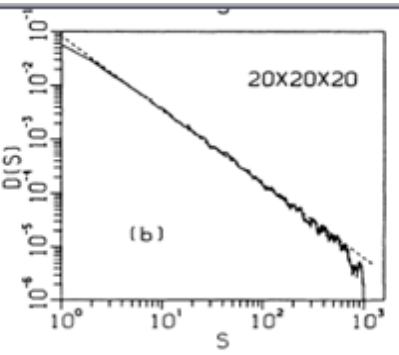

FIG. 3. Distribution of cluster sizes at criticality in two and three dimensions computed as described in the text. The data have been coarse grained. (a) 50×50 array, averaged over 200 samples. The dashed line is a straight line with slope -1.0; (b) $20 \times 20 \times 20$ array, averaged over 200 samples. The dashed straight line has a slope -1.37.

Time

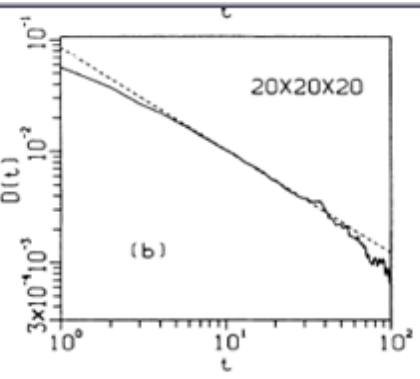

FIG. 4. Distribution of lifetimes corresponding to Fig. 3. (a) For the 50×50 array, the exponent $\alpha \approx 0.43$ yields a $1/f$ noise spectrum $f^{-1.57}$; (b) $20 \times 20 \times 20$ array, $\alpha \approx 0.92$, yielding an $f^{-1.08}$ spectrum.

SPATIOTEMPORAL CHAOS

Collective Dynamics and formation of structures in fluid flow from finite dimensional vortex structures to the **high dimensional turbulence**.

Defect Turbulence characterized by dynamical intermittency of regular and chaotic regions.

Intermittence turbulence is directly related to non-Gaussian dynamics. Deviation of probability distributions from Gaussian distributions is a signature for intermittency.

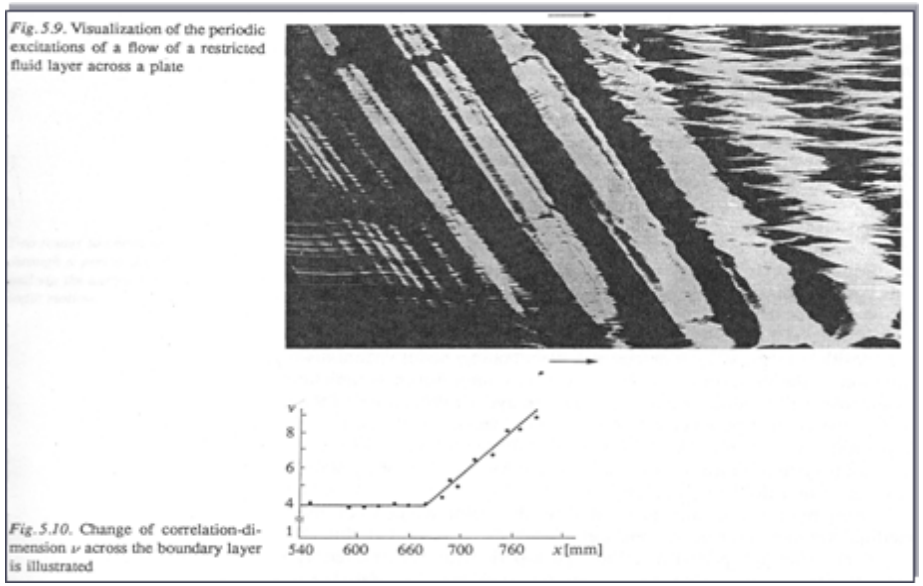

A.V. Gapanov et al. , 1992

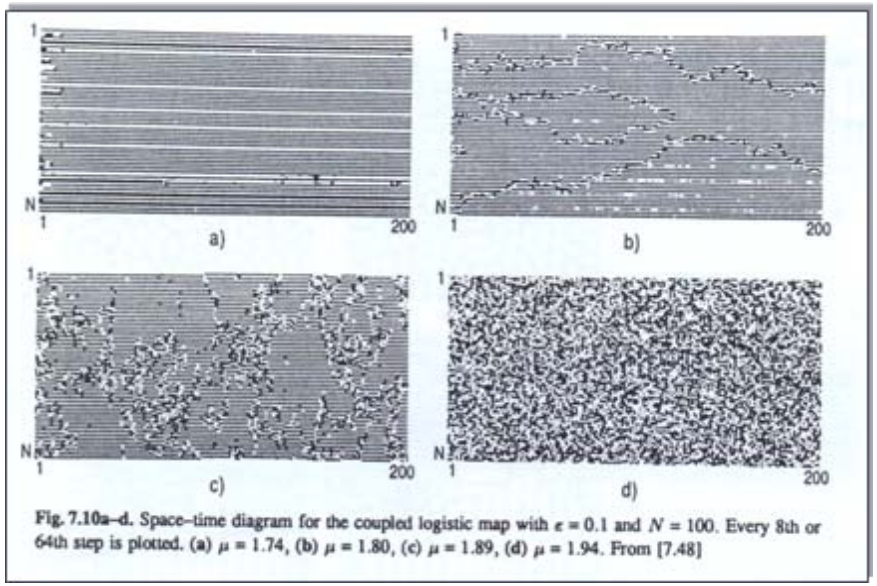

A.S. Michailov and and A. Yu.Loskutov , 1991

TWO CONTROVERSIAL THEORIES OF COMPLEXITY

SELF ORGANIZED CRITICALITY

- Many Degrees of Freedom (proportional to the size of the system) –Stochasticity
- Weak Chaos (Zero Lyapunov Exponent)
- Autonomous - Robust
- Impossible prediction

SANDPILE MODEL

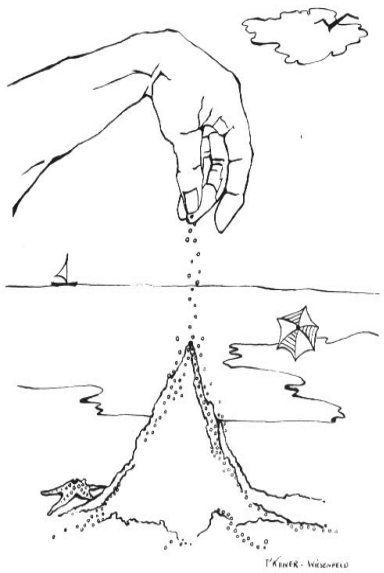

SPACE

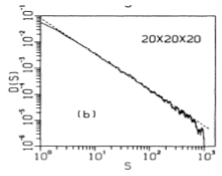

FIG. 3. Distribution of cluster sizes at criticality in two and three dimensions computed as described in the text. The data have been coarse grained. (a) 50×50 array, averaged over 200 samples. The dashed line is a straight line with slope −1.0; (b) 20×20×20 array, averaged over 200 samples. The dashed straight line has a slope −1.37.

TIME

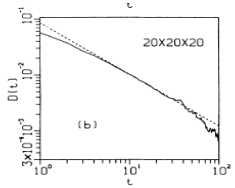

FIG. 4. Distribution of lifetimes corresponding to Fig. 3. (a) For the 50×50 array, the exponent $\alpha \approx 0.43$ yields a $1/f$ noise spectrum $f^{-1.57}$; (b) 20×20×20 array, $\alpha \approx 0.92$, yielding an $f^{-1.08}$ spectrum.

LOW DIMENSIONAL DETERMINISTIC CHAOS

- Few Degrees of Freedom - Determinism
- Strong Chaos – Sensitivity in Initial Conditions (one positive Lyapunov exponent)
- Control Parameters
- Short term prediction

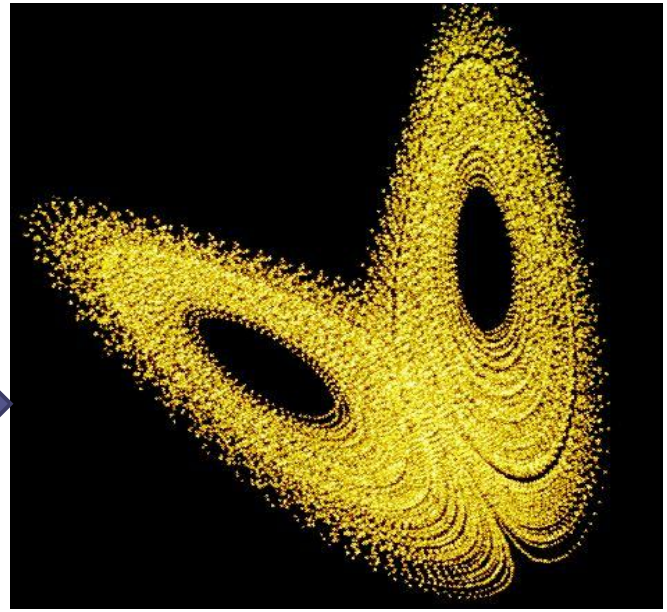

SOC & STRONG CHAOS COEXISTING

(M. de Souza Viera, 1996)

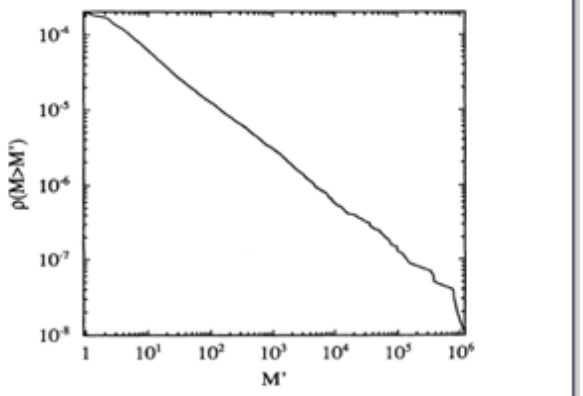

FIG. 1. Frequency of the avalanches $\rho(M > M')$ in which the displacement of the blocks M is greater than M'. The parameters are $\nu_c^{-1} = 0.8$, $\nu = 0.1$, and $N = 200$. The number of avalanches is 30 000 and $\rho(M > M')$ was divided by the number of blocks in the chain.

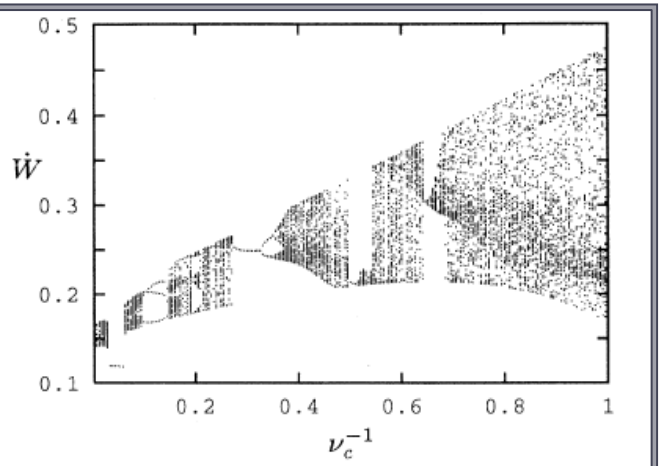

FIG. 2. Bifurcation diagram of the velocity of center of mass $\dot{W}$ on the surface of section $W = 0$ as a function of ν_c^{-1} for $\nu = 0.1$ and $N = 2$.

The nonlinear friction force will generate rich dynamics and **destroy SOC via chaotic behavior** as the parameters are changed.

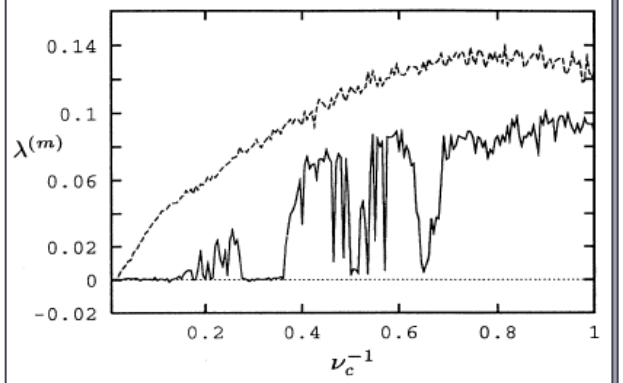

FIG. 3. The largest Liapunov exponent as a function of ν_c^{-1} with $\nu = 0.1$ for $N = 2$ (solid line), which corresponds to the bifurcation diagram shown in Fig. 2, and $N = 10$ (dashed line). The calculation of $\lambda^{(m)}$ is done for an integration time $\tau = 30\,000N$, with time steps of $\Delta\tau = 0.01$ and perturbations to the position and velocities of each block equal to 10^{-5}.

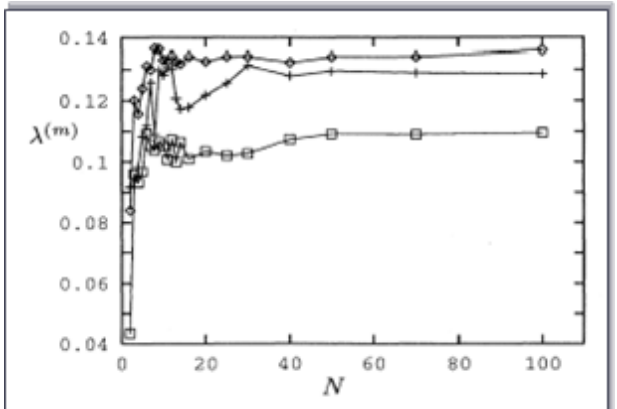

FIG. 4. The largest Liapunov exponent as a function of N for $\nu_c^{-1} = 0.8$ and $\nu = 0.1$ (diamonds), $\nu_c^{-1} = 0.8$ and $\nu = 0.01$ (crosses), $\nu_c^{-1} = 1.5$ and $\nu = 0.1$ (squares). As in Fig. 3, $\lambda^{(m)}$ is calculated for an integration time $\tau = 30\,000N$, with time steps of $\Delta\tau = 0.01$ and perturbations to the position and velocities of the blocks equal to 10^{-5}.

Theory of Chang

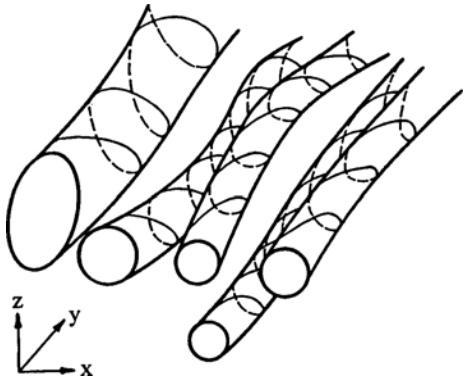

Coarse grained helicity

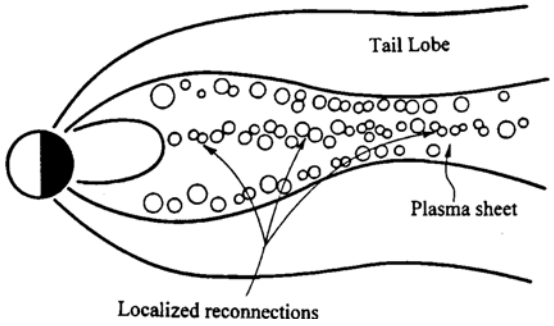

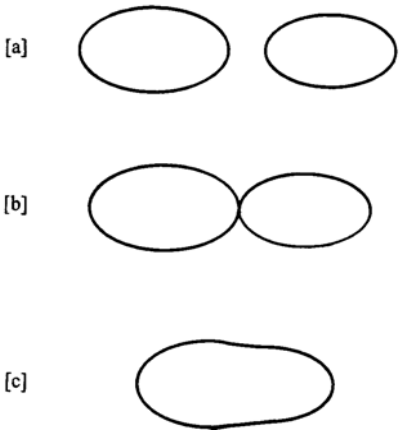

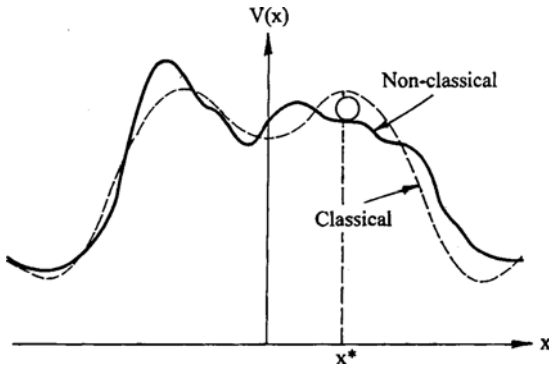

Intermittent Turbulence
Classical Instabilities
Non-Classical Instabilities
SOC

LOW – DIMENSIONAL BEHAVIOUR & SYMMETRY BREAKING OF STOCHASTIC SYSTEMS NEAR CRITICALITY

Using the concepts of the dynamic **renormalization group**, it can be demonstrated that nonlinear stochastic systems near **forced and/or SOC** can exhibit **low dimensional** and **fractal behavior.**

Generally, there exist a number of fixed points (singular points) in the flow field where the correlation length is infinite. Then the system is at criticality. The scaling laws for this regions exhibit multiple power or other nonlinear characteristics.

Fig.1

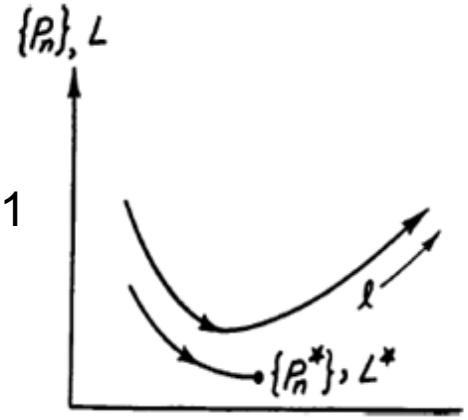

FIG. 5. Schematic representation of renormalization-group flow in the parameter space of the stochastic Lagrangian. Arrows indicate directions of increasing ℓ. There is a fixed point ($\partial L/\partial \ell = 0$) at L^*.

Fig.2

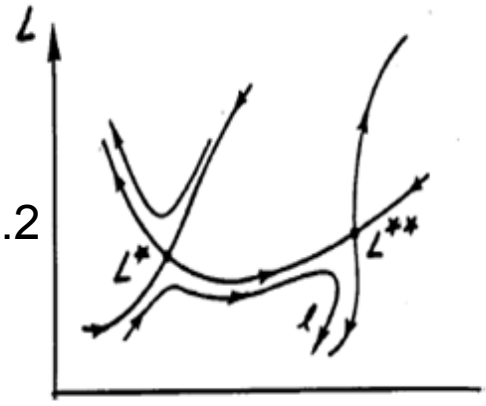

FIG. 6. Schematic representation of renormalization-group flow with two competing fixed points L^* and L^{**}. Arrows indicate directions of increasing ℓ.

Fig.3

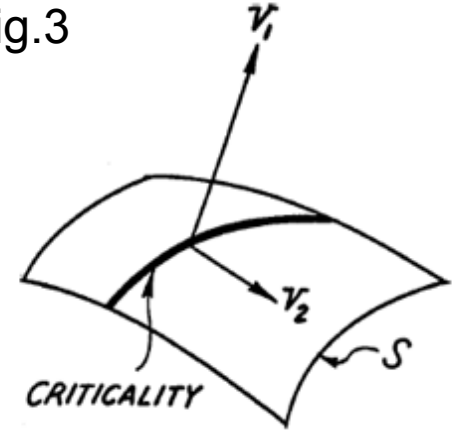

FIG. 7. Geometric representation of relevant scaling directions in an N-parameter affine space. S is an $(N-1)$-dimensional surface of constraint, and the heavy line represents an $(N-2)$-dimensional surface of criticality.

(Tom Chang, 1999)

Renormalization Group Theory (RGT)

$$\partial L / \partial l = RL$$

$$\partial L' / dl = R_L L' \qquad \text{ή}$$

$$dP_m^{'} / dl = \Sigma (R_L)_{mn} P_n^{'}$$

$$L'(l) = \Sigma V_k(l) U_k = \Sigma V_{k0} \exp(\lambda_k l) U_k$$

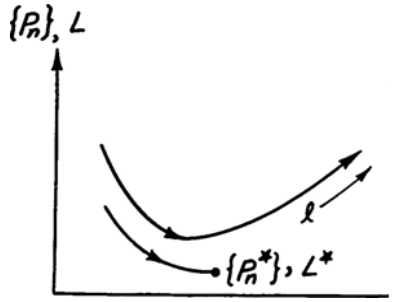

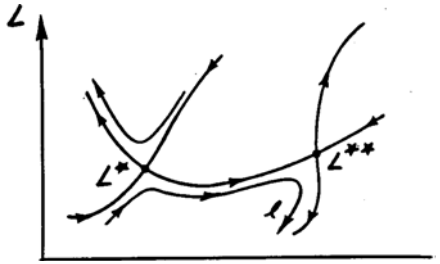

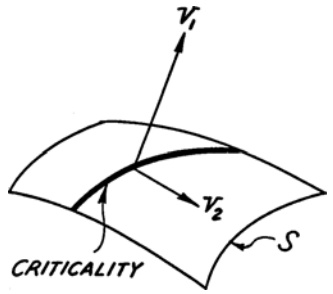

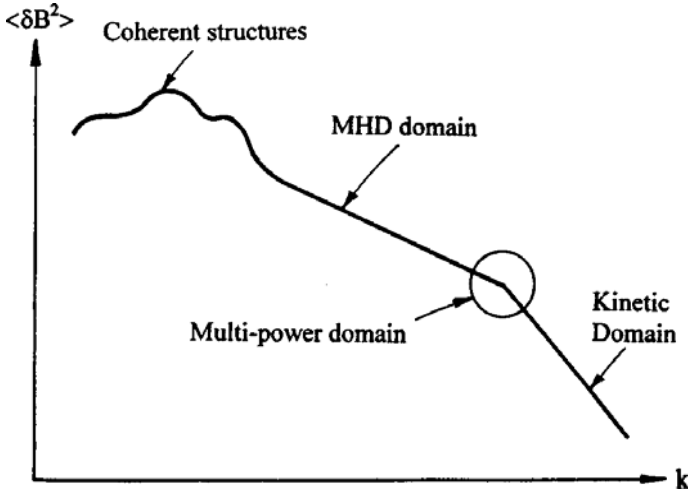

Breaking Symmetry – Bifurcation – Spectrum Fluctuations

THEORETICAL UNIFICATION OF FAR FROM EQUILIBRIUM SYSTEMS

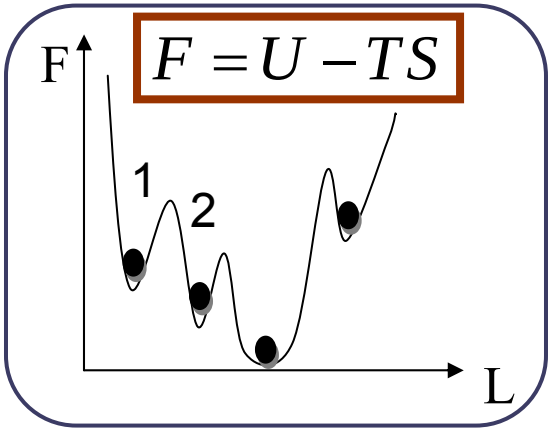

Εξάρτηση της συνάρτησης δυναμικού (Ελεύθερη Ενέργεια) από την παράμετρο L στον μετασχηματισμένο (configuration) χώρο

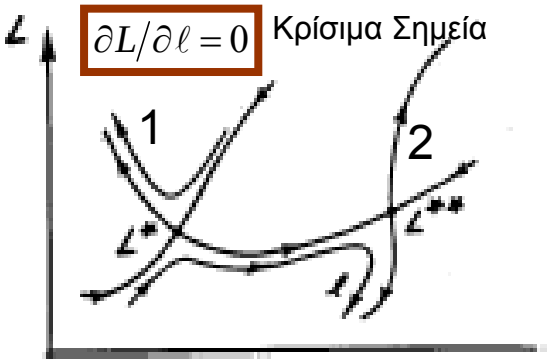

Σχηματική αναπαράσταση της ροής ομάδας επανακονικοποίησης με δύο ανταγωνιστικά ευσταθή σημεία, *L** και *L***. [Chang, 1999].

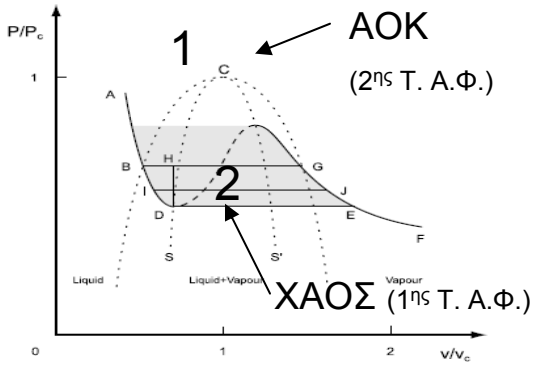

Μακριά από το κρίσιμο σημείο C, αλλαγές πρώτης τάξης . Στο κρίσιμο σημείο C αλλαγή φάσης δεύτερης τάξης. Απελευθέρωση ενέργειας με δύο διαφορετικούς τρόπους τοπικών ασταθειών (Rundle, 2003)

Langevin Εξίσωση

$$\frac{\partial \varphi_i}{\partial t} = f_i(\boldsymbol{\varphi}, \mathbf{x}, t) + n_i(\mathbf{x}, t)$$

Fokker-Planck Εξίσωση

$$P(\boldsymbol{\varphi}(\mathbf{x}, t)) = \int D(\boldsymbol{\varphi}) \exp\left\{-i \cdot \int L(\dot{\boldsymbol{\varphi}}, \boldsymbol{\varphi}, \mathbf{x})\, d\mathbf{x}\right\} dt$$

Επανακανονικοποίηση

$$\partial L/\partial \ell = \mathbf{R}L$$

$$\frac{dS}{dt} = \frac{dS_i}{dt} + \frac{dS_e}{dt} \leq 0$$

Μεταστατικές καταστάσεις μακριά από Θ.Ι.

Χωροχρονικές Δομές, ΑΟΚ, ΧΑΟΣ, Τύρβη κ.λ.π.

Boltzmann – Gibbs Statistics → *q* Gaussian Statistics (Tsallis Statistics)

Fractal topology and strange kinetics: from percolation theory to problems in cosmic electrodynamics

L M Zelenyĭ, A V Milovanov *Physics – Uspekhi* **47** (8) 749 – 788 (2004)

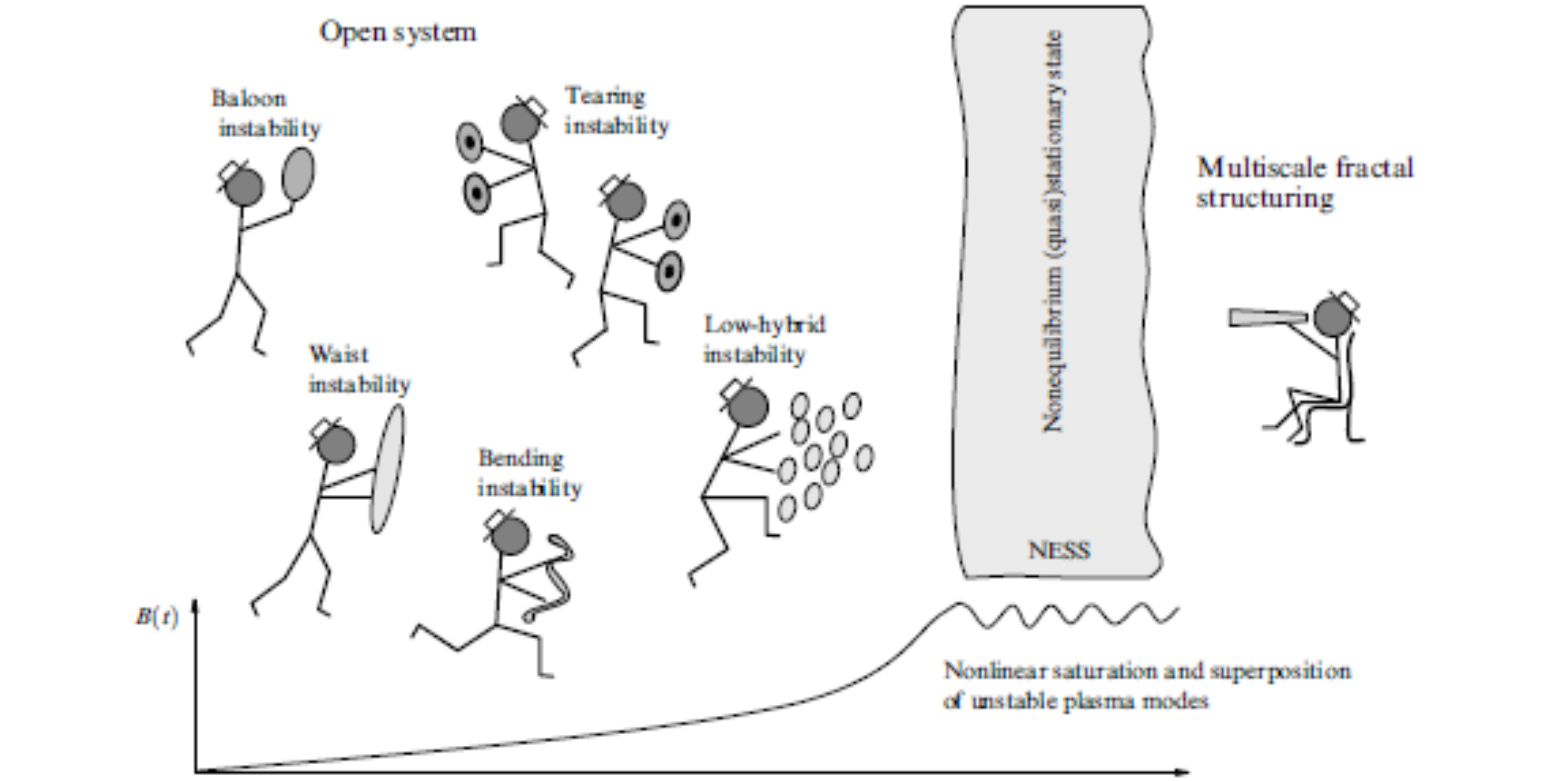

Figure 1. Development of a universal collective 'mode' corresponding to the transition of complex nonlinear dynamic systems towards a nonequilibrium (quasi)-stationary state. Examples are the processes of nonlinear stabilization and saturation of unstable plasma modes in the distant magnetotail of the earth (see Section 7 for more details). The characteristic dependence of the nonlinear amplitude of magnetoplasmic waves B on time is shown in the bottom part of the figure.

Linear Non-Linear Dynamics
Classical Physics (Particles and Fields)

$$\frac{\partial x}{\partial t} = f\left(x(\vec{r},t), \nabla, \nabla^2, \lambda\right)$$

$$\frac{\partial \rho(x,t)}{\partial t} = \hat{L}\rho(x,t)$$

Deterministic Process

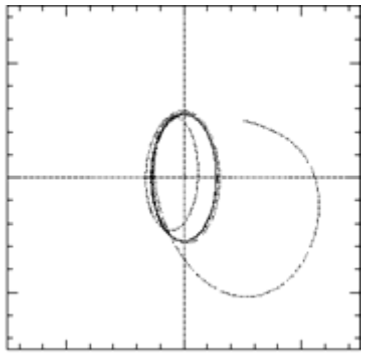

Forces - Trajectories

Liouville Process

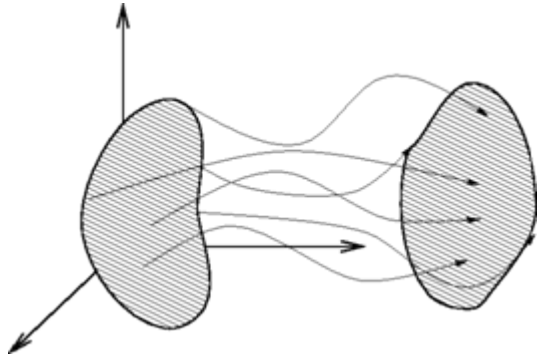

Ensemble Flows

Gaussian Statistical Mechanics

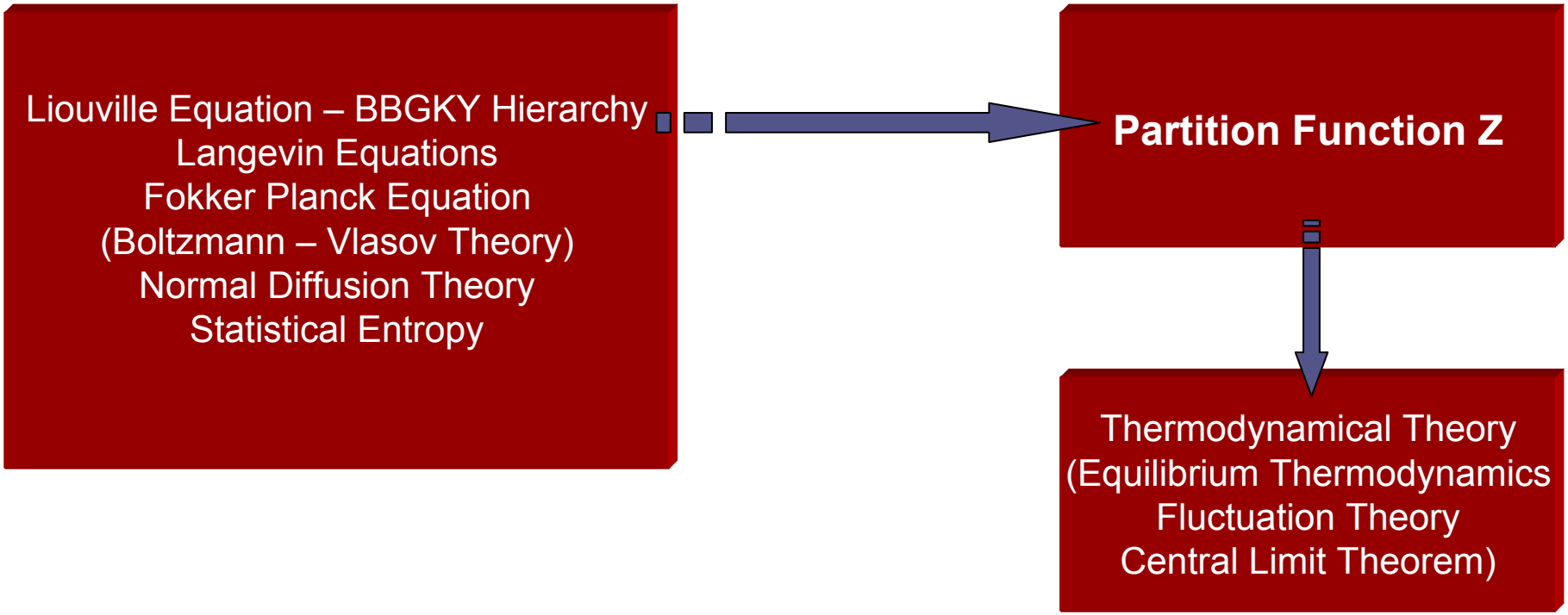

Langevin Equation $$dX_t = \mu(X_t, t)dt + \sqrt{2D(X_t, t)}dW_t$$

Fokker Planck Equation $$\frac{\partial}{\partial t}f(x,t) = -\frac{\partial}{\partial x}\left[\mu(x,t)f(x,t)\right] + \frac{\partial^2}{\partial x^2}\left[D(x,t)f(x,t)\right].$$

Turbulence – Intermittent Turbulence

Uriel Frisch – Turbulence (The Legacy of A.N. Kolmogorov)

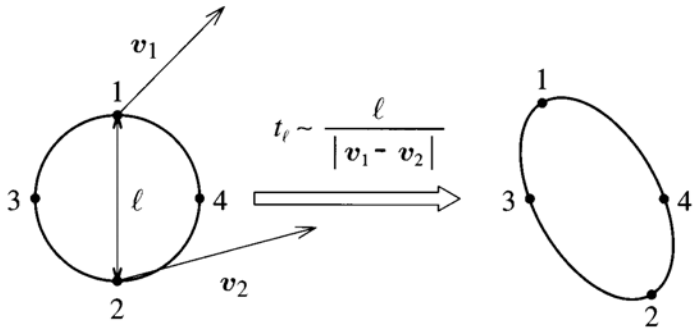

Fig. 7.1. Cross-section of a (roughly) spherical volume being squeezed into elliptical shape by fluid motion: points 1 and 2 separate, whilst points 3 and 4 get closer.

$$S_p(\ell) \equiv \langle (\delta v_\parallel(\ell))^p \rangle$$

$$S_p(x) \equiv \left\langle \left[\left(\boldsymbol{v}(\boldsymbol{r} + x\boldsymbol{\ell}^0) - \boldsymbol{v}(\boldsymbol{r}) \right) \cdot \boldsymbol{\ell}^0 \right]^p \right\rangle$$

$$S_p(\ell) \propto \ell^{p/3}.$$

$$S_p(\ell) = C_p \varepsilon^{p/3} \ell^{p/3}$$

'mother – eddy' ➔ 'daughters

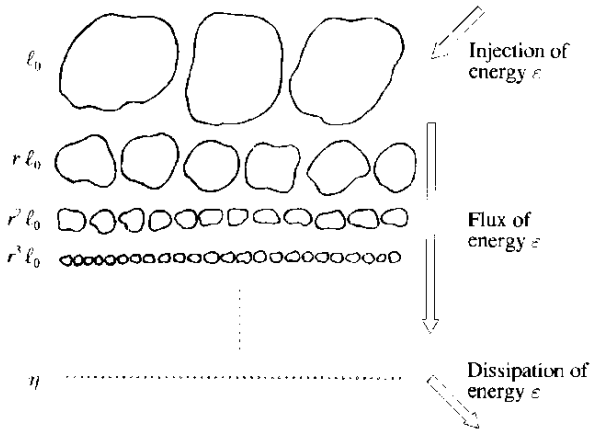

Fig. 7.2. The cascade according to the Kolmogorov 1941 theory. Notice that at each step the eddies are space-filling.

$$\Pi'_\ell \sim \frac{v_\ell^3}{\ell} \sim \varepsilon.$$

$$v_\ell \sim \varepsilon^{1/3} \ell^{1/3},$$

$$v_\ell \sim \sqrt{\langle \delta v_\parallel^2(\ell) \rangle},$$

$$t_\ell \sim \frac{\ell}{v_\ell}.$$

‘mother – eddy’ ➔ ‘daughters

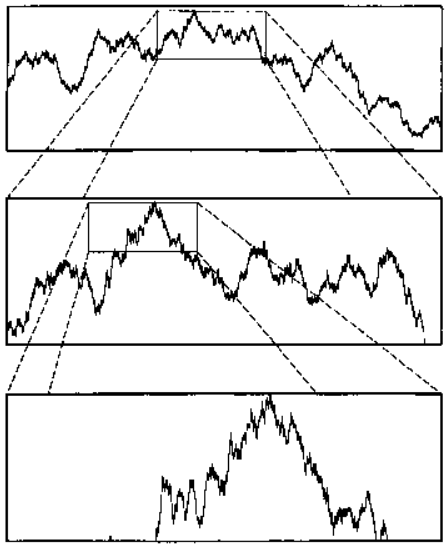

Fig. 8.1. A portion of the graph of the Brownian motion curve, enlarged t illustrating its self-similarity.

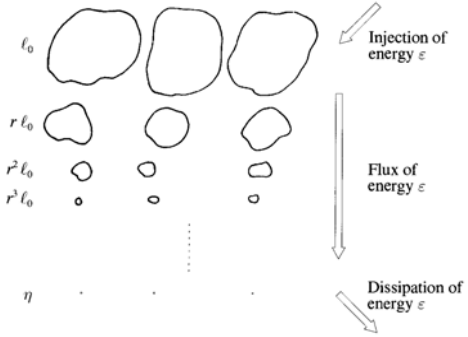

Fig. 8.9. The cascade according to the β-model. Notice that with each step the eddies become less and less space-filling.

(β-model)

$$\beta \ (0 < \beta < 1).$$

$$\ell = r^n \ell_0$$

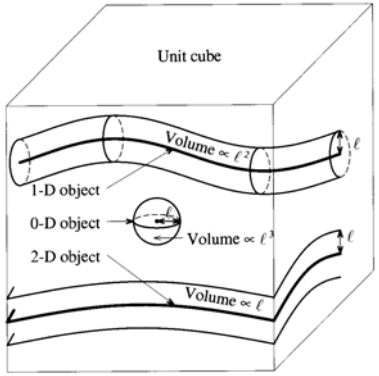

Fig. 8.10. The probability that a sphere of radius ℓ encounters an object of dimension D behaves as ℓ^{3-D} as $\ell \to 0$.

(probability density)

$$p_\ell = \beta^n = \beta^{\frac{\ln(\ell/\ell_0)}{\ln r}} = \left(\frac{\ell}{\ell_0}\right)^{3-D}$$

$$p_\ell \propto \ell^{3-D}, \qquad \ell \to 0.$$

$$p_\ell \propto \ell^{d-D}, \qquad \ell \to 0.$$

Multifractal intermittency velocity structure

Uriel Frisch – Turbulence (The Legacy of A.N. Kolmogorov)

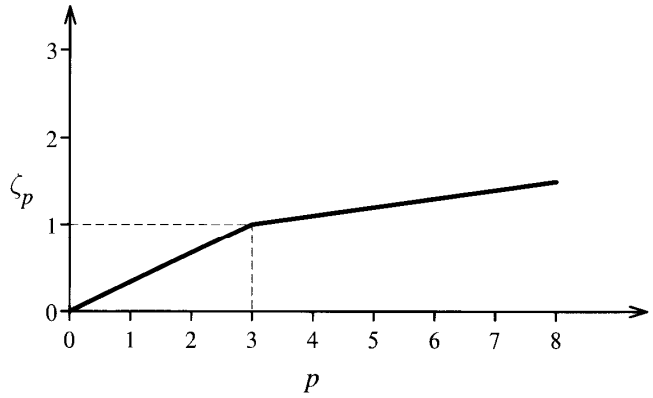

Fig. 8.11. Exponent ζ_p for the 'bifractal model'. Notice the change of slope at $p = 3$.

$$v_\ell \sim v_0 \left(\frac{\ell}{\ell_0}\right)^{\frac{1}{3}-\frac{3-D}{3}},$$

singular exponent $$h = \frac{1}{3} - \frac{3-D}{3}$$

$$S_p(\ell) = \langle \delta v_\ell^p \rangle \sim v_0^p \left(\frac{\ell}{\ell_0}\right)^{\zeta_p}$$

Bifractal β Model

$$\frac{\delta v_\ell(r)}{v_0} \sim \begin{cases} \left(\frac{\ell}{\ell_0}\right)^{h_1}, & r \in \mathcal{S}_1,\ \dim \mathcal{S}_1 = D_1 \\ \left(\frac{\ell}{\ell_0}\right)^{h_2}, & r \in \mathcal{S}_2,\ \dim \mathcal{S}_2 = D_2. \end{cases}$$

singularity manifold fractal set-fractal dimension

$$\langle \delta v_\ell^p \rangle \propto \ell^{\zeta_p}, \qquad \zeta_p = \min\left(ph_1 + 3 - D_1,\ ph_2 + 3 - D_2\right).$$

$$\zeta_p = \begin{cases} p/3 & 0 \le p \le 3 \\ p/3 + (3 - D_2)(1 - p/3) & p \ge 3. \end{cases}$$

multiscaling exponents spectrum

Multifractal β model

Uriel Frisch – Turbulence (The Legacy of A.N. Kolmogorov)

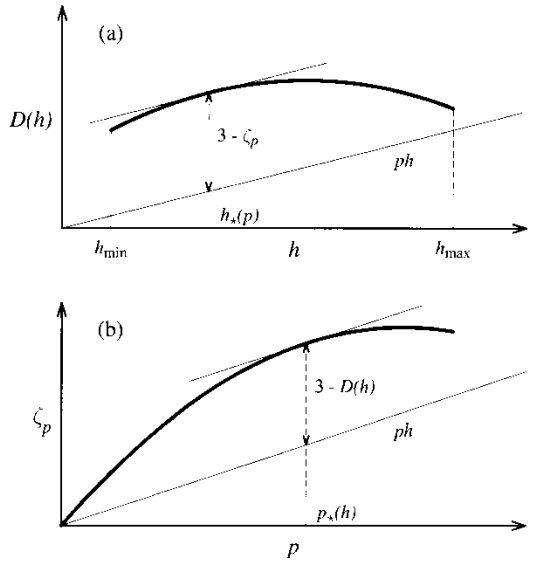

Fig. 8.13. Geometrical construction of the Legendre transform (a) and the inverse Legendre transform (b).

$$\frac{\delta v_\ell(\boldsymbol{r})}{v_0} \sim \left(\frac{\ell}{\ell_0}\right)^h, \qquad \boldsymbol{r} \in \mathcal{S}_h.$$

$$\frac{S_p(\ell)}{v_0^p} \equiv \frac{\langle \delta v_\ell^p \rangle}{v_0^p} \sim \int_I d\mu(h) \left(\frac{\ell}{\ell_0}\right)^{ph+3-D(h)}.$$

Legendre transformation

$$\lim_{\ell \to 0} \frac{\ln S_p(\ell)}{\ln \ell} = \zeta_p,$$

$$\zeta_p = \inf_h [ph + 3 - D(h)].$$

$$\frac{S_p(\ell)}{v_0^p} \sim \left(\frac{\ell}{\ell_0}\right)^{\zeta_p}, \qquad \ell \to 0.$$

$$\zeta_p = ph_\star(p) + 3 - D\left(h_\star(p)\right).$$

$$D'\left(h_\star(p)\right) = p,$$

$$D(h) = \inf_p \left(ph + 3 - \zeta_p\right).$$

$$\frac{d\zeta_p}{dp} = h_\star(p) + \left[p - D'\left(h_\star(p)\right)\right] \frac{dh_\star(p)}{dp} = h_\star(p)$$

$\mathbf{H}_{\mathbf{pmf}}$ *Under the same assumptions as in H1, there is a universal function $D(h)$ which maps real scaling exponents h to scaling dimensions $D \leq 3$ (including negative values and the value $-\infty$), such that for any h, the probability of velocity increments satisfies*

$$\lim_{\ell \to 0} \frac{\ln \bar{P}_\ell^{\text{inc}}\left(\pm \ell^h\right)}{\ln \ell} = 3 - D(h). \qquad (8.50)$$

Multifractal Intermittent Energy Dissipation

$$\varepsilon_\ell(\boldsymbol{r}) = \frac{1}{(4/3)\pi\ell^3}\int_{|\boldsymbol{r}'-\boldsymbol{r}|<\ell} d^3r'\frac{1}{2}\nu\sum_{ij}\left[\partial_j v_i(\boldsymbol{r}') + \partial_i v_j(\boldsymbol{r}')\right]^2$$

Definition. *The dissipation is said to be* multifractal *if there is a function* $F(\alpha)$ *which maps real scaling exponents* α *to scaling dimensions* $F \le 3$ *(including negative values and the value* $-\infty$*), such that for any* α

$$\lim_{\ell\to 0}\frac{\ln \bar{P}_\ell^{\mathrm{diss}}\left(\ell^{\alpha-1}\right)}{\ln \ell} = 3 - F(\alpha), \tag{8.79}$$

$$\left.\begin{aligned}\frac{\varepsilon_\ell(\boldsymbol{r})}{v_0^3/\ell_0} &\sim \left(\frac{\ell}{\ell_0}\right)^{\alpha-1} \quad \text{as } \ell\to 0,\\ \text{for } \quad \boldsymbol{r}\in\mathscr{D}_\alpha\subset\mathbb{R}^3;&\quad \dim\mathscr{D}_\alpha = F(\alpha).\end{aligned}\right\}$$

$$\langle\varepsilon_\ell^q\rangle \sim \left(\frac{v_0^3}{\ell_0}\right)^q\left(\frac{\ell}{\ell_0}\right)^{\tau_q}, \qquad \tau_q = \min_\alpha\left[q(\alpha-1)+3-F(\alpha)\right]$$

$$\varepsilon_\ell(x) \equiv \frac{1}{2\ell}\int_{|x'-x|<\ell} dx'\frac{1}{2}\nu\sum_{ij}\left[\partial_j v_i(x') + \partial_i v_j(x')\right]^2$$

$$\frac{\varepsilon_\ell(x)}{v_0^3/\ell_0} \sim \left(\frac{\ell}{\ell_0}\right)^{\alpha-1} \quad \text{as } \ell\to 0 \quad \text{for } \quad x\in\mathscr{D}'_\alpha; \qquad \dim\mathscr{D}'_\alpha = f(\alpha),$$

$$f(\alpha) \equiv F(\alpha) - 2.$$

Velocity – Energy Dissipation Multifractal Structures

$$h = \frac{\alpha}{3}, \qquad D(h) = F(\alpha) = f(\alpha) + 2, \qquad \zeta_p = \frac{p}{3} + \tau_{p/3}.$$

Space time scale envariance

$$\mathbf{r}' = \lambda\mathbf{r}, \quad \mathbf{u}' = \lambda^{\alpha/3}\mathbf{u}, \quad t' = \lambda^{1-\alpha/3}t, \quad (p/\rho)' = \lambda^{2\alpha/3}(p/\rho)\,.$$

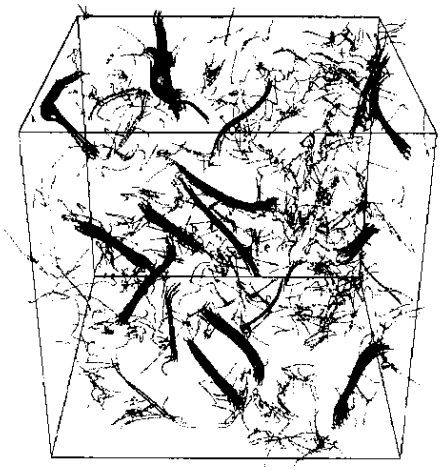

Fig. 7.4. Intermittent vortex filaments in a three-dimensional turbulent fluid simulated on a computer (She, Jackson and Orszag 1991).

Multifractal Theory

Theiler J., Vol. 7, No. 6/June 1990/J. Opt. Soc. Am. A, 1055

generalized dimensions

$$D_q = \frac{1}{q-1} \lim_{r \to 0} \frac{\log \sum_i P_i^q}{\log r}.$$

most-dence points

$$D_\infty = \lim_{r \to 0} \frac{\log\left(\max_i P_i\right)}{\log r},$$

least-dence points

$$D_{-\infty} = \lim_{r \to 0} \frac{\log\left(\min_i P_i\right)}{\log r}.$$

Information entropy

$$S(r) = -\sum_i P_i \log_2 P_i,$$

$$D_I = \lim_{r \to 0} \frac{-S(r)}{\log_2 r}$$

Information dimension

$$= \lim_{r \to 0} \frac{\sum_i P_i \log_2 P_i}{\log_2 r}.$$

Rényi entropy

$$S_q(r) = \frac{1}{q-1} \log \sum_i P_i^q,$$

$$D_q = \lim_{r \to 0} \frac{-S_q(r)}{\log r} = \frac{1}{q-1} \lim_{r \to 0} \frac{\log \sum_i P_i^q}{\log r},$$

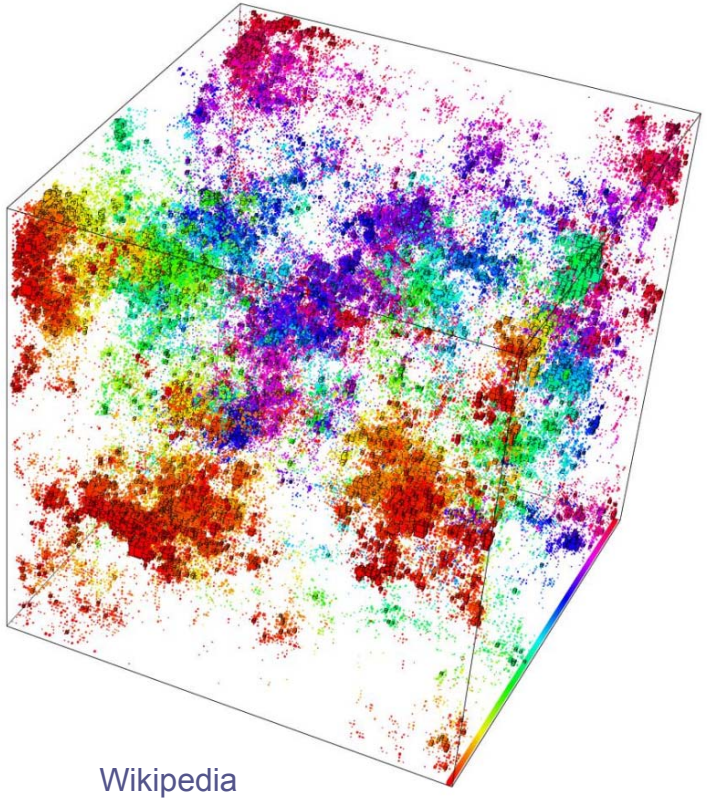

Wikipedia

Multifractal Theory

Theiler J., Vol. 7, No. 6/June 1990/J. Opt. Soc. Am. A, 1055

$$P_i = r^{\alpha} \qquad n(\alpha, r) \sim r^{-f(\alpha)} \Delta\alpha.$$

$$\sum_i P_i^q = \int n(\alpha, r) r^{q\alpha} \mathrm{d}\alpha \qquad \theta = \min_\alpha \{q\alpha - f(\alpha)\}$$

$$\sim \int r^{-f(\alpha)} r^{q\alpha} \mathrm{d}\alpha \sim r^{\theta},$$

$$\sum_i P_i^q \sim r^{(q-1)D_q},$$

$$\alpha = \frac{\partial \tau}{\partial q} \qquad f = \alpha q - \tau$$

and

$$q = \frac{\partial f}{\partial \alpha} \qquad \tau = \alpha q - f.$$

$$f(\alpha) = \min_q \{q\alpha - \tau(q)\},$$

$$\tau(q) = \min_\alpha \{q\alpha - f(\alpha)\}.$$

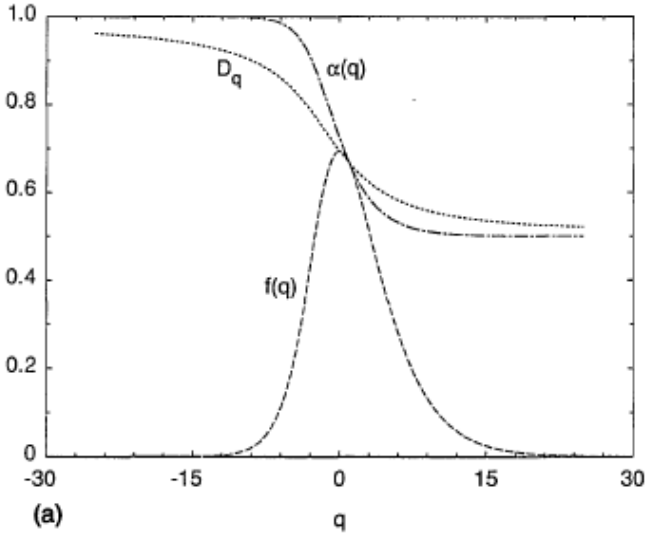

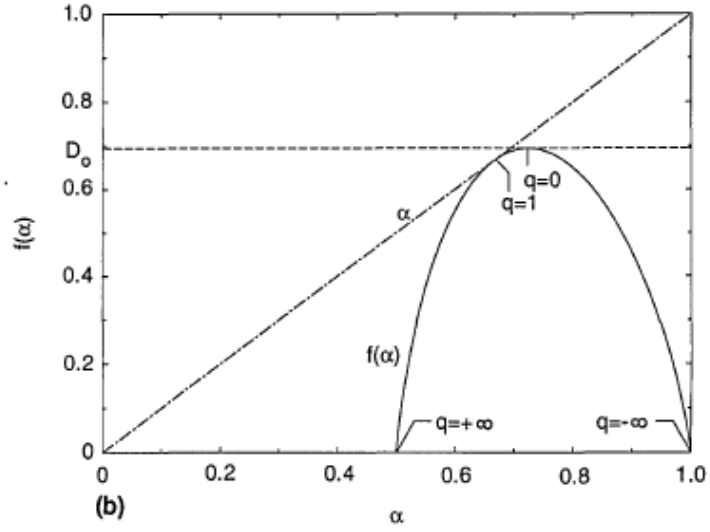

Tsallis Theory
Nonextensive Statistical Mechanics

$$S_q = k \ln_q W \quad (S_1 = S_{BG}). \qquad S_q = k \langle \ln_q (1/p_i) \rangle . \qquad S_q = k \frac{1 - \sum_{i=1}^{W} p_i^q}{q-1} .$$

$$y = [1 + (1-q)x]^{1/(1-q)} \equiv e_q^x \quad (e_1^x = e^x). \qquad \frac{dy}{dx} = y^q \qquad y = \frac{x^{1-q} - 1}{1-q} \equiv \ln_q x \quad (x > 0;\ \ln_1 x = \ln x),$$

$$\frac{S_q(A+B)}{k} = \frac{S_q(A)}{k} + \frac{S_q(B)}{k} + (1-q)\frac{S_q(A)}{k}\frac{S_q(B)}{k}. \qquad S_q[A+B] = S_q[A] + S_q[B|A] + (1-q)S_q[A]S_q[B|A],$$

Generalized Fokker-Planck Equations

$$\frac{\partial^\beta p(x,t)}{\partial |t|^\beta} = D_{\beta,\gamma,q} \frac{\partial^\gamma [p(x,t)]^{2-q}}{\partial |x|^\gamma} \quad (0 < \beta \le 1; 0 < \gamma \le 2).$$

$$\frac{\partial p(x,t)}{\partial t} = D_{\gamma,q} \frac{\partial^\gamma [p(x,t)]^{2-q}}{\partial |x|^\gamma} \quad (0 < \gamma \le 2; q < 3).$$

$$L_\gamma(x) \propto \frac{1}{|x|^{1+\gamma}} \quad (|x| \to \infty; 0 < \gamma < 2), \qquad \text{Levy Distribution}$$

$$p_q(x) \propto \frac{1}{|x|^{2/(q-1)}} \quad (|x| \to \infty;\ 1 < q < 3). \qquad \text{q-Gaussian Distribution}$$

$$\gamma = \begin{cases} 2 & \text{if } q \le 5/3, \\ \frac{3-q}{q-1} & \text{if } 5/3 < q < 3, \end{cases}$$

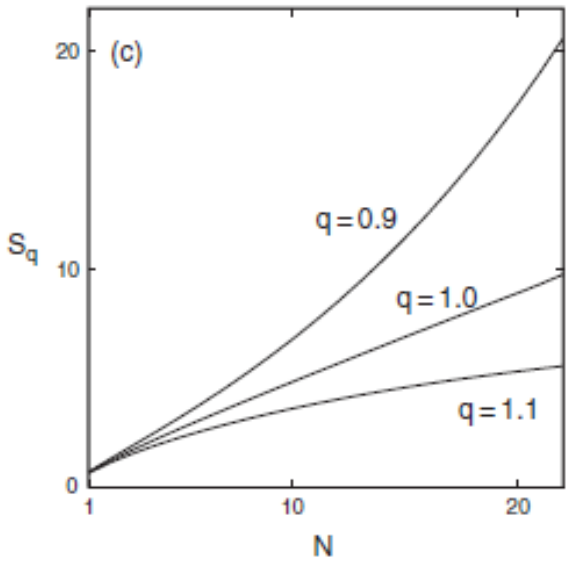

q-extension of thermodynamics

$$Z_q = \sum_{conf} e_q^{-\beta q(E_i - V_q)}$$

$$\beta_q = \beta / \sum_{conf} p_i^q \qquad \beta = 1/KT$$

$$\langle E \rangle_q \equiv \sum_{conf} p_i^q E_i / \sum_{conf} p_i^q = U_q$$

$$F_q \equiv U_q - TS_q = -\frac{1}{\beta} \ln qZ_q$$

$$U_q = \frac{\partial}{\partial \beta} \ln qZ_q, \frac{1}{T} = \frac{\partial S_q}{\partial U_q}$$

$$C_q \equiv T \frac{\partial \delta_q}{\partial T} = \frac{\partial U_q}{\partial T} = -T \frac{\partial^2 F_q}{\partial T^2}$$

q-extension of central limit theorem

q-independent random variables

$$F_q[X+Y](\xi) = F_q[X](\xi) \otimes_{\frac{1+q}{3-q}} F_q[Y](\xi), \qquad F_q[f](\xi) \equiv \int dx\, e_q^{i\xi x} \otimes_q f(x).$$

where $h(x, y)$ is the joint distribution. Therefore, *q-independence* means *independence* for $q = 1$ (i.e., $h(x, y) = f_X(x) f_Y(y)$), and it means *strong correlation* (of a certain class) for $q \neq 1$ (i.e., $h(x, y) \neq f_X(x) f_Y(y)$).

The q-triplet of Tsallis

Gaussian-BG equilibrium (qstat=qsen=qrel=1) → Nonequilibrium (qstat, qsen, qrel)

$\frac{dy}{dx} = y^q$, $(y(0)=1, q \in \Re)$ → (qstat, qsen, qrel)

Equilibrium PDF → Metaequilibrium PDF

(qstat) $\frac{d(p_i Z_{stat})}{dE_i} = -\beta q_{stat} (p_i Z_{stat})^{q_{stat}}$ → $p(x) \propto \left[1-(1-q)\beta_{q_{stat}} x^2\right]^{1/1-q_{stat}}$

Equilibrium BG entropy production → Metaequilibrium q-entropy production

(qsen) $K_q \equiv \lim_{t\to\infty} \lim_{W\to\infty} \lim_{N\to\infty} \frac{<S_q>(t)}{t}$ → $\frac{1}{1-q_{sen}} = \frac{1}{\alpha_{min}} - \frac{1}{\alpha_{max}}$ $\quad f(a_{min}) = f(a_{max}) = 0$

$\frac{d\xi}{dt} = \lambda_{q_{sen}} \xi^{q_{sen}}$, → $\xi = e_{q_{sen}}^{\lambda_{q_{sen}} t}$, $\quad \xi \equiv \lim_{\Delta x(0)\to 0} \frac{\Delta x(t)}{\Delta x(0)}$,

Equilibrium relaxation process → Metaequilibrium nonextensive relaxation process

(qrel) $\Omega(t) \equiv [O(t) - O(\infty)] / [O(0) - O(\infty)]$ $\frac{d\Omega}{dt} = -\frac{1}{T_{q_{rel}}} \Omega^{q_{rel}}$ → $\Omega(t) \simeq e_{q_{rel}}^{-t/\tau_{rel}}$

Intermittent Turbulence – Tsallis Theory

$$\varepsilon_n \sim \varepsilon_0 \left(l_n / l_0\right)^{\alpha-1}$$

$$\sum_n \varepsilon_n^q l_n^d \sim l_n^{(q-1)D_n} = l_n^{\tau(q)}$$

$$dn(\alpha) \sim l_n^{-f_d(\alpha)} d\alpha$$

$$f_d(a) = a\bar{q} - (\bar{q}-1)(D_{\bar{q}} - d + 1) + d - 1$$

$$a = \frac{d}{d\bar{q}}[(\bar{q}-1)(D_{\bar{q}} - d + 1)]$$

$$f(a) = a\bar{q} - \tau(\bar{q}),$$

$$a = \frac{d}{d\bar{q}}[(q-1)D_q] = \frac{d}{d\bar{q}}\tau(\bar{q})$$

$$\bar{q} = \frac{df(a)}{da}$$

- multi=-fractal and multi-scale diffusion in the physical space

$$P(a) = Z_q^{-1}[1-(1-q)\frac{(a-a_0)^2}{2X/\ln 2}]^{\frac{1}{1-q}}$$

$$Z_q = \sqrt{2X/[(1-q)\ln 2]}$$

- Theoretical Estimation (Arimitsu, Arimitsu)

$$f(a) = D_0 + \log_2[1-(1-q)\frac{(a-a_o)^2}{2X/\ln 2}]/(1-q)^{-1}$$

$$\tau(\bar{q}) = \bar{q}a_0 - 1 - \frac{2X\bar{q}^2}{1+\sqrt{C_{\bar{q}}}} - \frac{1}{1-q}[1-\log_2(1+\sqrt{C_{\bar{q}}})]$$

$$a_{\bar{q}} - a_0 = (1-\sqrt{C_{\bar{q}}})/[\bar{q}(1-q)\ln 2]$$

$$q = 1-a \qquad \frac{1}{1-q} = \frac{1}{a_-} - \frac{1}{a_+}$$

- Spectrum of Structure Functions

$$Sp(l^n) = <|\delta u_n|^p>$$

$$J(p) = 1 + \tau(\bar{q} = \frac{p}{3})$$

$$J(p) = \frac{a_0 p}{3} - \frac{2Xp^2}{q(1+\sqrt{C_{p/3}})} - \frac{1}{1-q}[1-\log_2(1+\sqrt{C_{p/3}})]$$

$$J(p) = \frac{p}{3} + T^{(u)}(p) + T^{(F)}(p)$$

$$S(2) \equiv <\varepsilon^2/\varepsilon> \delta_n^{\mu} = \delta_n^{J(2)} \dashrightarrow \mu = J(2)$$

$$P(f) \sim f^{-5/3} \dashrightarrow P(f) \sim f^{-(5/3+\mu)}$$

Strange kinetics

Michael F. Shlesinger, George M. Zaslavsky & Joseph Klafter NATURE · VOL 363 · 6 MAY 1993

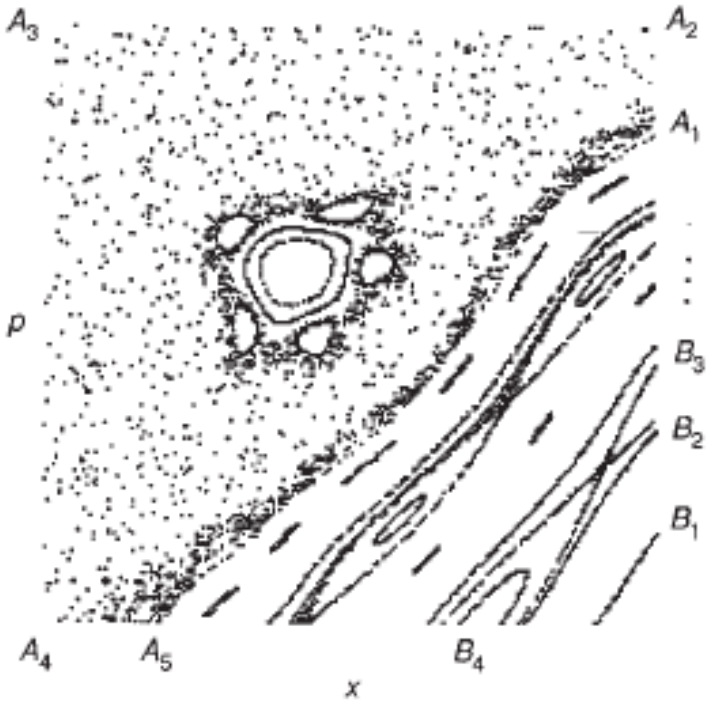

FIG. 1 Illustration of the topology of dynamical system orbits in the phase space (x, p). Starting from some initial conditions, the orbit is generated by an infinite set of iterations, equation (2), and each iteration gives a dot on the (x, p) plane. Such a procedure is called a Poincaré section. Instead of a continuous curve, the orbit is represented on the (x, p) plane by the set of values (x_n, p_n) taken at special set of time instants. We plot a typical part of the (x, p) plane for equation (2) with $K_0=1.2$. The regular orbits $(B_1, B_2, B_3, B_4, \ldots)$ describe quasiperiodic motion. In contrast to them, there is an orbit which fills the domain $A=(A_1, A_2, A_3, A_4, A_5)$ (except for some area in its central part). There is no possibility of fitting all of these points onto one curve. This orbit represents chaotic motion. The area A is a 'stochastic sea'. Inside A there is a set of 'islands' in which the motion is regular. Domain A borders a big island along the curve A_5A_1 (there is only a part of the island in the figure and the orbits $B_1, B_2, \ldots$ are closed in this island). The density of points in the 'stochastic sea' area (or distribution function) displays how often this part of the phase space has been visited. The density is inhomogeneous and the most visited parts are narrow strips close to island boundaries. Dark strips of high density points are distributed along the border (A_1A_5) of the big island, around the smaller island and its five satellite sub-islands.

$$\langle R^2(t)\rangle \sim t^{\gamma}$$

$$\langle |R| \rangle \sim t^{\mu} \qquad (t \to \infty)$$

$$p_n(k) = \exp\left(-\text{constant} \times n|k|^{\alpha}\right)$$

$$p_n(x) \sim \text{constant} \times n/x^{1+\alpha}$$

$$\mathscr{R} = \lim_{\Delta t \to 0, \Delta x \to 0} |\Delta x|^{2\alpha}/|\Delta t|^{\beta} = \text{constant}$$

FRACTIONAL KINETIC EQUATION
(FRACTIONAL FOKKER–PLANCK–KOLMOGOROV EQUATION)

Zaslavsky G.M., Chaos, fractional kinetics, and anomalous transport, *Physics Reports 371, 461-580*, 2002.

$$\frac{\partial^\beta P(x,t)}{\partial t^\beta} = \frac{\partial^\alpha}{\partial(-x)^\alpha}(\mathscr{A}(x)P(x,y)) + \frac{\partial^{\alpha_1}}{\partial(-x)^{\alpha_1}}(\mathscr{B}(x)P(x,y))$$

$$\mathscr{B}(x) = \frac{1}{\Gamma(2+\alpha)} \lim_{\Delta t \to 0} \frac{\langle\langle |\Delta x|^{\alpha+1} \rangle\rangle}{(\Delta t)^\beta} ,$$

$$\mathscr{A}(x) = \frac{1}{\Gamma(1+\alpha)} \lim_{\Delta t \to 0} \frac{\langle\langle |\Delta x|^{\alpha} \rangle\rangle}{(\Delta t)^\beta}$$

$$\langle R^2(t) \rangle \sim t^\gamma$$

$$p_n(k) = \exp\left(-\text{constant} \times n|k|^\alpha\right)$$

$$p_n(x) \sim \text{constant} \times n/x^{1+\alpha}$$

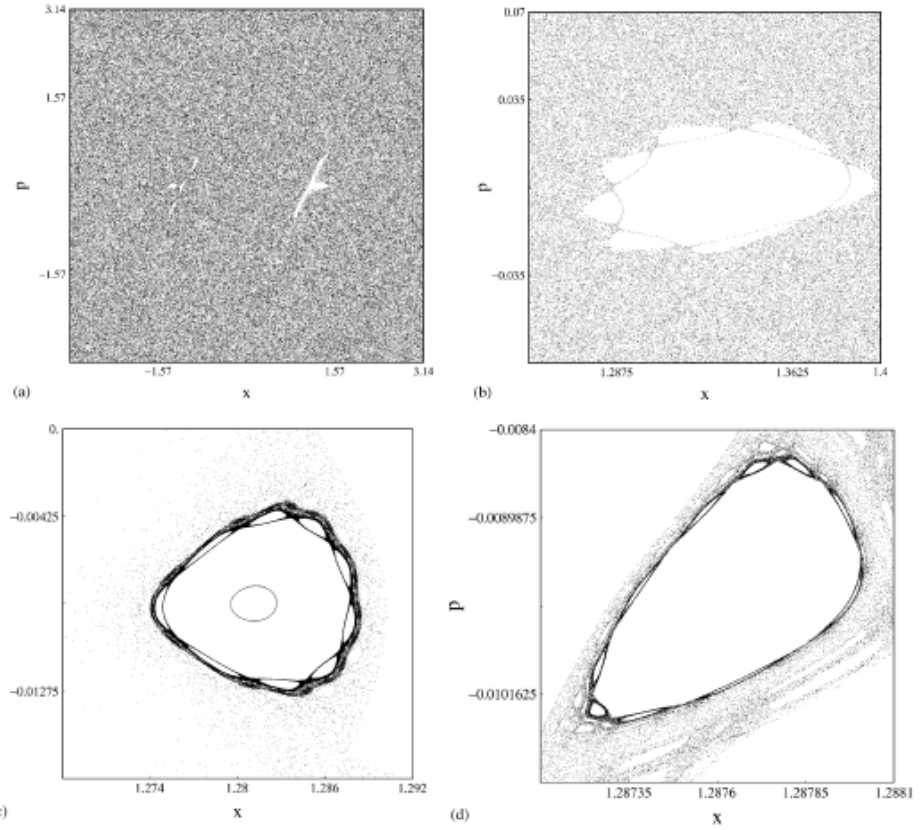

FRACTIONAL INTEGRAL MAXWELL EQUATIONS

Tarasov V., Electromagnetic field of fractal distribution of charged particles, arXiv, arXiv:physics/0610010, 2006.

Using the fractional generalization of Stokes's and Gauss's theorems (see Appendix), we can rewrite the fractional integral Maxwell equations in the form

$$\int_W c_3^{-1}(D,\mathbf{r}) div(c_2(d,\mathbf{r})\mathbf{E}) dV_D = \frac{1}{\varepsilon_0}\int_W \rho dV_D,$$

$$\int_S c_2^{-1}(d,\mathbf{r})(curl(c_1(\gamma,\mathbf{r})\mathbf{E}), d\mathbf{S}_d) = -\frac{\partial}{\partial t}\int_S (\mathbf{B}, d\mathbf{S}_d),$$

$$\int_W c_3^{-1}(D,\mathbf{r}) div(c_2(d,\mathbf{r})\mathbf{B}) dV_d = 0,$$

$$\int_S c_2^{-1}(d,\mathbf{r})(curl(c_1(\gamma,\mathbf{r})\mathbf{B}), d\mathbf{S}_d) = \mu_0\int_S (\mathbf{J}, d\mathbf{S}_d) + \varepsilon_0\mu_0\frac{\partial}{\partial t}\int_S (\mathbf{E}, d\mathbf{S}_d),$$

As a result, we have the following differential Maxwell equations:

$$div\Big(c_2(d,\mathbf{r})\mathbf{E}\Big) = \frac{1}{\varepsilon_0} c_3(D,\mathbf{r})\rho,$$

$$curl\Big(c_1(\gamma,\mathbf{r})\mathbf{E}\Big) = -c_2(d,\mathbf{r})\frac{\partial}{\partial t}\mathbf{B},$$

$$div\Big(c_2(d,\mathbf{r})\mathbf{B}\Big) = 0,$$

$$curl\Big(c_1(\gamma,\mathbf{r})\mathbf{B}\Big) = \mu_0 c_2(d,\mathbf{r})\mathbf{J} + \varepsilon_0\mu_0 c_2(d,\mathbf{r})\frac{\partial \mathbf{E}}{\partial t}.$$

$$c_1(\gamma,\mathbf{r}) = \frac{2^{1-\gamma}\Gamma(1/2)}{\Gamma(\gamma/2)}|\mathbf{r}|^{\gamma-1}. \qquad dS_d = c_2(d,\mathbf{r})dS_2, \quad c_2(d,\mathbf{r}) = \frac{2^{2-d}}{\Gamma(d/2)}|\mathbf{r}|^{d-2}. \qquad dV_D = c_3(D,\mathbf{r})dV_3. \qquad c_3(D,\mathbf{r}) = \frac{2^{3-D}\Gamma(3/2)}{\Gamma(D/2)}|\mathbf{r}|^{D-3}.$$

FRACTIONAL LIOUVILLE EQUATION FOR N-PARTICLE SYSTEM

Tarasov V., *Journal of Physics: Conference Series* **7**, *17–33*, 2005

we can derive the fractional Liouville equation [10] for N-particle distribution function in the form

$$\frac{d\tilde{\rho}_N}{dt} + \Omega_\alpha \tilde{\rho}_N = 0, \tag{26}$$

The omega function Ω_α is defined by the equation

$$\Omega_\alpha = \sum_{k=1}^{N} \sum_{a=1}^{n} \Big(\{K_a^k, p_{ka}^\alpha\}_\alpha + \{q_{ka}^\alpha, F_a^k\}_\alpha \Big). \tag{28}$$

Here we use the following notations for the brackets

$$\{A, B\}_\alpha = \sum_{k=1}^{N} \sum_{a=1}^{n} \Big(\frac{\partial A}{\partial q_{ka}^\alpha} \frac{\partial B}{\partial p_{ka}^\alpha} - \frac{\partial A}{\partial p_{ka}^\alpha} \frac{\partial B}{\partial q_{ka}^\alpha} \Big). \tag{29}$$

Using Eqs. (26), (28) and (27), we can rewrite the Liouville equation in the equivalent form

$$\frac{\partial \tilde{\rho}_N}{\partial t} = \mathcal{L}_N \tilde{\rho}_N, \tag{30}$$

where $\mathcal{L}_N$ is Liouville operator that is defined by the equation

$$\mathcal{L}_N \tilde{\rho}_N = - \sum_{k=1}^{N} \Big(\frac{\partial (\mathbf{K}_k \tilde{\rho}_N)}{\partial \mathbf{q}_k^\alpha} + \frac{\partial (\mathbf{F}_k \tilde{\rho}_N)}{\partial \mathbf{p}_k^\alpha} \Big). \tag{31}$$

Here we use definition of 2-particle distribution function $\tilde{\rho}_2$. This distribution is defined by the fractional integration of the N-particle distribution function over all $\mathbf{q}_k$ and $\mathbf{p}_k$, except $k = 1, 2$:

$$\tilde{\rho}_2 = \tilde{\rho}(\mathbf{q}_1, \mathbf{p}_1, \mathbf{q}_2, \mathbf{p}_2, t) = \hat{I}^\alpha[3, ..., N] \tilde{\rho}_N(\mathbf{q}, \mathbf{p}, t). \tag{77}$$

The fractional generalization of 1-particle reduced distribution function $\tilde{\rho}_1$ can be defined by the equation

$$\tilde{\rho}_1(\mathbf{q}, \mathbf{p}, t) = \tilde{\rho}(\mathbf{q}_1, \mathbf{p}_1, t) = \hat{I}^\alpha[2, ..., N] \tilde{\rho}_N(\mathbf{q}, \mathbf{p}, t). \tag{67}$$

Therefore the fractional generalization of the first BBGKI equation has the form

$$\frac{\partial \tilde{\rho}_1}{\partial t} = \mathcal{L}_1 \tilde{\rho}_1 + I(\tilde{\rho}_2),$$

FRACTAL GENERALIZATION OF MAGNETOHYDRODYNAMICS (MHD) EQUATIONS

Tarasov V., Magnetohydrodynamic of Fractal Media, arXiv,arXiv:0711.0305, 2007.

(1) The equation of continuity,

$$\left(\frac{d}{dt}\right)_D \rho = -\rho \nabla_k^D u_k.$$

(2) The equation of balance of density of momentum,

$$\rho \left(\frac{d}{dt}\right)_D u_k = \rho f_k - \nabla_k^D p.$$

(3) Faraday's law,

$$curl\Big(c_1(\gamma, \mathbf{r})\mathbf{E}\Big) = -c_2(d, \mathbf{r})\frac{\partial}{\partial t}\mathbf{B}.$$

(4) The absence of magnetic monopoles

$$div\Big(c_2(d, \mathbf{r})\mathbf{B}\Big) = 0.$$

(5) Ampere's law,

$$curl\Big(c_1(\gamma, \mathbf{r})\mathbf{B}\Big) = \mu_0 c_2(d, \mathbf{r})\mathbf{J},$$

Fractal topology and strange kinetics: from percolation theory to problems in cosmic electrodynamics

L M Zelenyĭ, A V Milovanov *Physics – Uspekhi* **47** (8) 749 – 788 (2004)

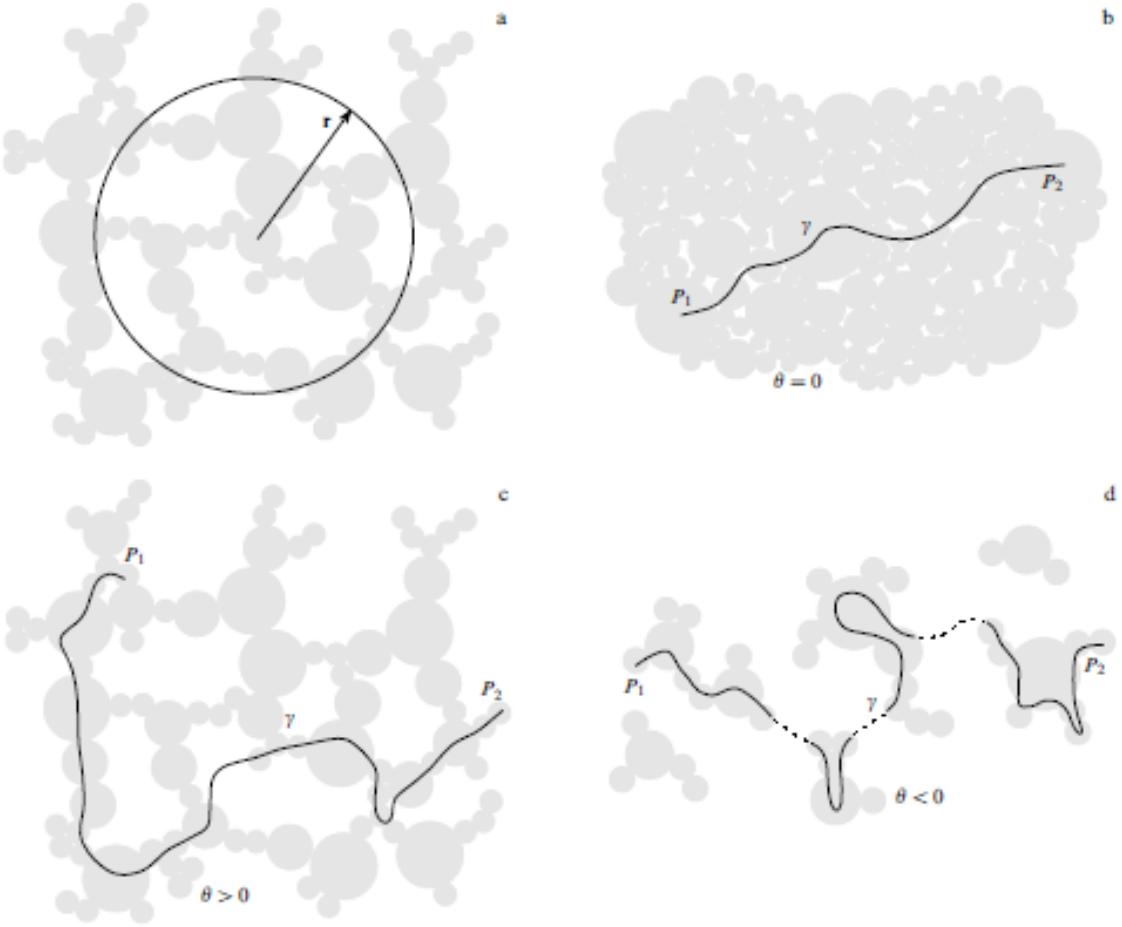

Figure 3. (a) Definition of the Hausdorff dimension d_f. The number of the fractal structural elements inside a hypersphere of radius r is proportional to r^{d_f}. Definition of the connectivity index: (b) $\theta = 0$, the Hausdorff dimension of the geodesic γ connecting points P_1 and P_2 is equal to one; (c) $\theta > 0$, the Hausdorff dimension of the geodesic γ connecting points P_1 and P_2 is necessarily greater than one; (d) $\theta < 0$, the geodesic γ connecting points P_1 and P_2 is everywhere discontinuous and its Hausdorff dimension is strictly less than one.

Fractional Kinetic Equation

L M Zelenyĭ, A V Milovanov *Physics – Uspekhi* **47** (8) 749 – 788 (2004)

$$\frac{\partial^{\alpha}\psi}{\partial t^{\alpha}} = \nabla_{\mathbf{r}}^{2\beta}(\mathcal{B}\psi)\,.$$

$$\frac{\partial^{\alpha}}{\partial t^{\alpha}}\,\psi(t,\mathbf{r}) = \frac{1}{\Gamma(m-\alpha)}\,\frac{\partial^{m}}{\partial t^{m}}\int_{0}^{t}\frac{\mathrm{d}\vartheta}{(t-\vartheta)^{1+\alpha-m}}\,\psi(\vartheta,\mathbf{r})\,,$$

$$\frac{\partial^{\beta}}{\partial x_i^{\beta}}\,\psi(t,\mathbf{r}) = \frac{1}{\Gamma(1-\beta)}\,\frac{\partial}{\partial x_i}\int_{-\infty}^{x_i}\frac{\mathrm{d}x_i'}{(x_i - x_i')^{\beta}}\,\psi(t,\mathbf{r}')\,.$$

Solar Photosphere

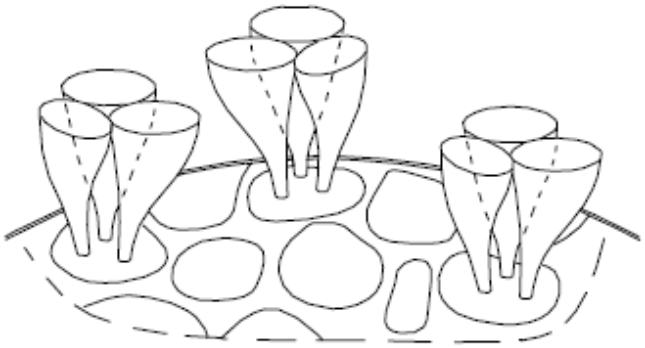

Figure 19. The roots of intense flux tubes are continuously shuffled by multi-scale convective flows forming hierarchical fractal structures in the solar photosphere.

Solar Wind

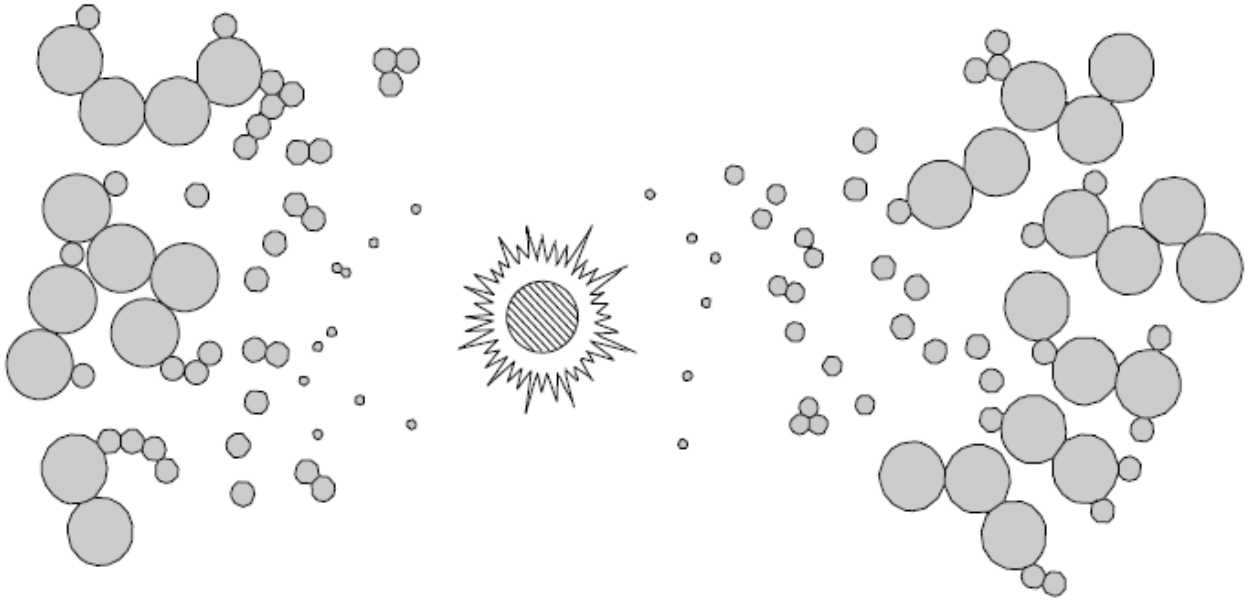

Figure 18. The aggregation of intense flux tubes of the interplanetary magnetic field. The inflation of tubes is due to the dynamic pressure drop in the solar wind outflowing from the corona.

Fractal topology and strange kinetics: from percolation theory to problems in cosmic electrodynamics

L M Zelenyĭ, A V Milovanov *Physics – Uspekhi* **47** (8) 749 – 788 (2004)

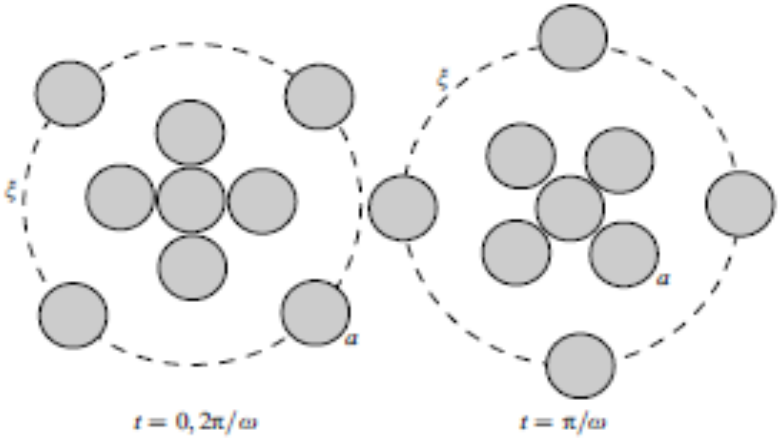

Figure 21. Fractons are vibrations of fractal blobs. Examples are collective harmonic oscillations of turbulent magnetic field clots around some common equilibrium point. Shown are the states of the clots separated by the oscillation half-period, $\Delta t = \pi/\omega$.

$$\frac{i\partial\Psi(t,x)}{\partial t} = i^{-\alpha}\Lambda\nabla_x^\alpha\Psi(t,x) + \mathcal{D}_\beta\nabla_{-x}^\beta\nabla_x^\beta\Psi(t,x) - \zeta|\Psi(t,x)|^2\Psi(t,x). \qquad (11.28)$$

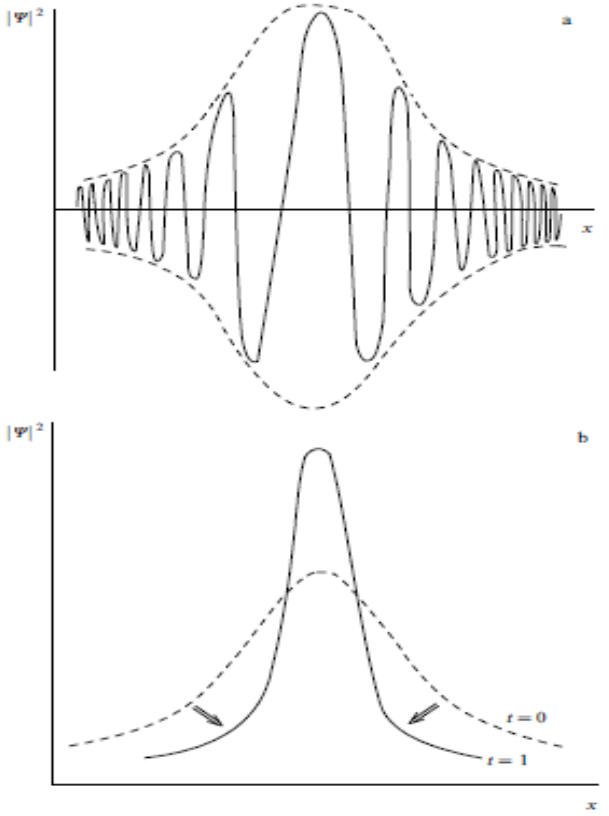

Figure 22. (a) The principal averaged nonlinear effect manifested as fracton oscillations increase is the dependence of the excitation frequency ω on the amplitude $|\Psi(t,x)|^2$. For $\zeta > 0$, the oscillation frequency in the tail exceeds the corresponding value in the central part of the fracton. The envelope of the nonlinear fracton mode is shown by the dashed line. (b) The development of the modulation instability leads to gradual energy transmission from the tail to the core of the fracton excitation. Shown is the position of the envelope at two successive moments of time $t = 0$ and $t = 1$. The phenomenon can be treated as a self-focusing (or self-squeezing) of the nonlinear fracton mode.

Tsallis statistics and magnetospheric self-organization

G.P. Pavlos [a], L.P. Karakatsanis [a,*], M.N. Xenakis [a], D. Sarafopoulos [a], E.G. Pavlos [b]

Physica A 391 (2012) 3069–3080

$$\dot{\Psi}_i = -\Gamma \frac{\delta F}{\delta \Psi_i} + N_i$$

$$\left\langle N_i\left(\vec{x}, t\right) N\left(\vec{x}', t'\right)\right\rangle = 2\Gamma\left(\vec{x}\right)\delta_{ij}\delta\left(\vec{x}-\vec{x}'\right)\delta\left(t-t'\right)\Psi_i\left(\vec{x}, t\right)$$

Generalized Langevin Equation

$$G_N^q\left(\vec{x}_1, \vec{x}_2, \ldots, \vec{x}_N\right) = \left\langle \Psi\left(\vec{x}_1\right) \cdot \Psi\left(\vec{x}_2\right) \cdot \ldots \cdot \Psi\left(\vec{x}_N\right)\right\rangle = \frac{1}{2}\int D[\Psi] \cdot \Phi\left(\vec{x}_1\right) \cdot \Phi\left(\vec{x}_2\right) \cdot \ldots \cdot \Phi\left(\vec{x}_N\right) \cdot e^{-\int Fq\, d^D x}$$

$$Z\left(J\left(\vec{x}\right)\right) = \int D[\Psi] \cdot e^{-\int Fq J\, d^D x}$$

$$Z_q = \lim_{J \to 0} Z\left(J\left(\vec{x}\right)\right).$$

N-point correlation function G_N and q-partition functions

$$G_N^q\left(\vec{x}_1, \vec{x}_2, \ldots, \vec{x}_N\right) = \frac{1}{Z}\frac{\delta^N Z_q\left(J\left(\vec{x}\right)\right)}{\delta J\left(\vec{x}_1\right) \cdot \delta J\left(\vec{x}_2\right) \cdot \ldots \cdot \delta J\left(\vec{x}_N\right)}.$$

Scale invariance principle

$$\vec{K}^n = R_l\left(\vec{K}^{n-1}\right) = \cdots = R_l^n \cdot \left(\vec{K}^0\right), \quad n = 0, 1, 2, \ldots,$$

RG transformation

$$\xi\left(\vec{K}^n\right) = l^{-1} \cdot \xi\left(\vec{K}^{n-1}\right) = \cdots = l^{-n} \cdot \xi\left(\vec{K}^0\right).$$

At the fixed points $\vec{K}^*$ of the RG flow, the relation:

$$\xi\left(\vec{K}^*\right) = l^{-1} \cdot \xi\left(\vec{K}^*\right)$$

Critical - fixed points

THANK YOU
for your attention